

## CRISPR/Cas9 mutated *p*-coumaroyl shikimate 3'-hydroxylase 3 gene in *Populus tomentosa* reveals lignin functioning on supporting tree upright

Sufang Zhang<sup>a</sup>, Bo Wang<sup>b</sup>, Qian Li<sup>a</sup>, Wenkai Hui<sup>a</sup>, Linjie Yang<sup>c</sup>, Zhihua Wang<sup>a</sup>, Wenjuan Zhang<sup>a</sup>, Fengxia Yue<sup>c</sup>, Nian Liu<sup>a</sup>, Huiling Li<sup>a</sup>, Fachuang Lu<sup>c,d</sup>, Kewei Zhang<sup>e</sup>, Qingyin Zeng<sup>f,\*</sup>, Ai-Min Wu<sup>a,\*</sup>

<sup>a</sup> Guangdong Key Laboratory for Innovative Development and Utilization of Forest Plant Germplasm, College of Forestry and Landscape Architectures, South China Agricultural University, Guangzhou 510642, China

<sup>b</sup> College of Agriculture, South China Agricultural University, Guangzhou 510642, China

<sup>c</sup> State Key Laboratory of Pulp and Paper Engineering, School of Light Industry and Engineering, South China University of Technology, Guangzhou 510640, China

<sup>d</sup> Department of Biochemistry and Great Lakes Bioenergy Research Center, The Wisconsin Energy Institute, University of Wisconsin, Madison, WI 53726, USA

<sup>e</sup> College of Chemistry and Life Sciences, Zhejiang Normal University, Jinhua, Zhejiang 321004, China

<sup>f</sup> State Key Laboratory of Tree Genetics and Breeding, Chinese Academy of Forestry, Beijing 100091, China



### ARTICLE INFO

#### Keywords:

*c3'h3* mutant  
Secondary metabolism  
Lignin  
Dwarf  
Flavonoid  
*Populus tomentosa*

### ABSTRACT

The lignin plays one of the most important roles in plant secondary metabolism. However, it is still unclear how lignin can contribute to the impressive height of wood growth. In this study, *C3'H*, a rate-limiting enzyme of the lignin pathway, was used as the target gene. *C3'H3* was knocked out by CRISPR/Cas9 in *Populus tomentosa*. Compared with wild-type popular trees, *c3'h3* mutants exhibited dwarf phenotypes, collapsed xylem vessels, weakened phloem thickening, decreased hydraulic conductivity and photosynthetic efficiency, and reduced auxin content, except for reduced total lignin content and significantly increased H-subunit lignin. In the *c3'h3* mutant, the flavonoid biosynthesis genes *CHS*, *CHI*, *F3H*, *DFR*, *ANR*, and *LAR* were upregulated, and flavonoid metabolite accumulations were detected, indicating that decreasing the lignin biosynthesis pathway enhanced flavonoid metabolic flux. Furthermore, flavonoid metabolites, such as naringenin and hesperetin, were largely increased, while higher hesperetin content suppressed plant cell division. Thus, studying the *c3'h3* mutant allows us to deduce that lignin deficiency suppresses tree growth and leads to the dwarf phenotype due to collapsed xylem and thickened phloem, limiting material exchanges and transport.

### 1. Introduction

*Populus* spp. is one of the most widely distributed and adaptable fast-growing tree species in the world. Poplar wood is an important lignocellulosic raw material characterized by rapid growth and vigorous reproductive capabilities. It is also a crucial resource for papermaking, construction, and energy [1]. The cell wall serves as not only a physical barrier and the first line of defense between plant cells and the external environment but also a flexible structure that regulates plant growth [2]. The upward growth and transpiration of terrestrial plants pose challenges to water transport capacity. Water is transported from the roots to the leaves through the xylem, and xylem damage hinders water transport [3]. The water transport capacity of the xylem is determined by the unique structure of its cell wall, particularly the secondary cell wall.

Lignin, the second most abundant component of lignocellulose, plays a significant role in mechanical support, water and inorganic salt transportation, and defense against plant diseases and insect pests [4]. Therefore, there is a need to appropriately regulate monolignols or enzymes involved in the lignin biosynthesis process.

As we all know, lignin is mainly composed of *p*-hydroxyphenyl (H), guaiacyl (G), and syringyl (S) subunits, which are derived from three phenylpropanoid alcohols: *p*-coumaryl, coniferyl, and sinapyl alcohol. These alcohols are also known as monolignols [5,6]. Genes associated with genetic modifications of lignification usually result in reducing the content of lignin, changing its composition, and affecting plant growth and development [7–11]. Lignin biosynthesis emerged from the ancestral general phenylpropanoid metabolism, which became established in early terrestrial plants when they migrated from water to land

\* Corresponding authors.

E-mail addresses: [qingyin.zeng@ibcas.ac.cn](mailto:qingyin.zeng@ibcas.ac.cn) (Q. Zeng), [wuaimin@scau.edu.cn](mailto:wuaimin@scau.edu.cn) (A.-M. Wu).

approximately 500 million years ago [12].

In the monolignol pathway, C3H is a cytochrome P450-dependent monooxygenase that catalyzes the formation of caffeoyl shikimate by hydroxylating p-coumaroyl shikimate. It is considered one of the most conserved gene families and first appeared in moss [13]. Previously, de Vries et al. [14] described the detection of C3H in all land plants and one putative C3H ortholog in *K. nitens*. The algal sequences showed strong divergence from the C3Hs, forming only a larger streptophyte-specific clade with CYP450 enzymes [15]. Additionally, C3H is absent in algae and only exists in land plants (embryophytes). Lignin endowed early tracheophytes with the physical rigidity to stand upright and strengthened the water-conducting cells for long-distance water transport. Lignification consequently transformed phenylpropanoid metabolism into a major carbon sink in plants, eclipsed only by cellulose [12]. However, with the evolution's progression, only one C3H exists in one species in moss or ferns, with the exception of *Physcomitrella patens* [15]. C3'H (Coumaroyl shikimate 3'-Hydroxylase) is a rate-limiting enzyme gene in the phenylpropanoid class of the lignin biosynthetic pathway, which controls the direction of carbon supply flow to lignin monomers [16]. Although C3'H is known to play a role in lignin biosynthesis in many plants, gaps between secondary cell wall lignin and plant growth remain unclear, especially in wood. In the *Populus*, there are four members of C3H clast. Therefore, in here by knocking out the highest expressed C3'H gene in poplar wood, whether the mutants would exhibit dwarf appearance as atavism due to loss of lignin.

## 2. Results

### 2.1. Phylogenetic analysis of lignin genes in woody

To study the function of lignin in woody plants, a phylogenetic analysis of three cytochrome P450 monooxygenases, namely C3H, C4H (cinnamate 4-hydroxylase), and F5H (ferulate 5-hydroxylase), was conducted in 25 plant species. The occurrence of C3H in ferns and mosses was very rare, with only one identified in most species except for *Physcomitrella patens*. The presence of C4H was also limited, and no F5H genes were found in ferns and mosses. However, angiosperms (such as *Populus trichocarpa*, *Eucalyptus grandis*, and *Phyllostachys edulis*) exhibited a higher number of C3H and F5H genes compared to gymnosperms (*Picea abies* and *Pinus taeda*). Additionally, no C3H genes were identified in green algae (*Volvox carteri*, *Chlamydomonas reinhardtii*, *Chlorella variabilis*, *Ostreococcus tauri*, *Micromonas pusilla*) and red algae (*Cyanidioschyzon merolae*, *Porphyra umbilicalis*, *Porphyridium purpureum*), indicating lignin pathway genes might be important for evolutions from aquatic plants to terrestrial plants (Fig. 1a). The aligned C3H, C4H, and F5H homologs by a maximum likelihood phylogeny (Fig. S1) displayed independent cluster each other.

C3'H, belonging to the CYP98A family among cytochrome P450 enzymes, occupies a crucial regulatory position in the lignin biosynthetic pathway [17–19]. To explore the evolutionary and phylogenetic relationships of C3'H members in different species, a phylogenetic tree was constructed (Fig. 1b). The phylogenetic analysis of C3'H among various species clearly categorized them into three groups: mosses and ferns, gymnosperms, and angiosperms. Families within the same group usually clustered closely together, with only a few exceptions. Several species were confirmed to possess the C3'H gene, including mosses (*Physcomitrella patens*, *Sphagnum fallax*, *Marchantia polymorpha*), ferns (*Selaginella moellendorffii*, *Azolla filiculoides*, *Salvinia cucullata*), gymnosperms (*Picea abies*, *Pinus taeda*), and angiosperms (*Populus trichocarpa*, *Eucalyptus grandis*, *Amborella trichopoda*, *Solanum lycopersicum*, *Asparagus officinalis*, *Oryza sativa*, *Phyllostachys edulis*, *Nymphaea colorata*, *Arabidopsis*) (Fig. 1b). In poplar, four homologous genes of C3'H (*PtrC3'H1*, *PtrC3'H2*, *PtrC3'H3*, and *PtrC3'H4*) were identified, exhibiting close genetic proximity. Furthermore, the genetic distance of C3'H members in *Populus trichocarpa* and *Eucalyptus grandis* was the closest, suggesting a strong relationship between broad-leaved tree (Fig. 1b).

### 2.2. Loss of lignin in c3'h3 mutant showed dwarf phenotype

To identify high-expression genes, the transcript levels of the four C3'H homologous genes were determined using RT-qPCR. The expression levels of C3'H3 were significantly higher in the xylem, phloem, apical, middle, and basal parts of the stem compared to the other three C3'H genes (Fig. 2a), consistent with previous reports which C3'H3 is highly expressed in the xylem [20,21], suggesting that C3'H3 may play a major role in wood lignin production.

To study exact C3'H functions on lignin in wood, the C3'H3 gene was selected and modified with single and three target CRISPR/Cas9 sites, and then introduced into *P. tomentosa*. Although the single-target sequence was identical to the third target sequence of the three-target CRISPR/Cas9 construct, none of the c3'h3 mutants were identified from the single-target construct. However, two independent c3'h3 homozygous mutants were obtained from the three-target CRISPR/Cas9 constructs in 14 transgenic lines (Fig. 2b, c). The results revealed numerous mutations, including deletions (–) and insertions (+), at the three sgRNA-targeted sites of the two independent c3'h3 homozygous mutants. A 26-bp deletion occurred in Target 3 and a 6-bp deletion occurred in the Target 1 site of c3'h3-1, while a 4-bp deletion occurred in the Target 1 site of c3'h3-2 (Fig. 2c). These deletions resulted in translational frameshifts or premature termination of C3'H3. To avoid off-target effects, we sequenced all three other C3'H genes and confirmed that only C3'H3 was mutated. Surprisingly, in all transgenic trees, the secondary target was not mutated, indicating target sequences were important in tree CRISPR/Cas9 system for mutants.

One-month-old c3'h3 mutant and wild-type seedlings were transplanted into soil with a plastic hood. The c3'h3 mutant plants barely grew, whereas the wild type continuously thrived (Fig. 2b). If we opened the hood, the leaves of the c3'h3 mutant plants withered and died after 4 h, whereas the wild type grew normally (Data S1). Over time, the leaf size of the wild type gradually increased and eventually became stable, with a constant increase in plant height. However, the leaf sizes and plant heights of the two c3'h3 mutant lines were significantly lower than those of the wild type at different times (Fig. 2d-f). Through microscopic observation, significant changes in cell morphology were found (Fig. 2g, h) and a significant reduction in cell perimeter and surface area were detected (Fig. 2i, j). Xylem vessels are important for water transport. Therefore, the water potential of the wild type and c3'h3 mutants was measured, and the results showed that the water potential of c3'h3 mutants was significantly lower than that of the wild type (Fig. 2k). Since the two mutant lines had completely identical phenotypes and growth patterns, we selected only c3'h3-1 for further analysis.

### 2.3. Reduction of photosynthetic capability in loss of lignin by c3'h3 mutant

Considering that the c3'h3 mutants were dwarfs and their growth was almost stagnant, their photosynthetic capabilities were determined. The fluorescence values of Y (NA), ETR (II), NPQ, and qL in c3'h3 mutant leaves were significantly lower than those of the WT (Table S1). Additionally, ETR (I), Y (I), and Y (NA) from PSI were also reduced, especially Y (NA) (Table S1). The results of chlorophyll fluorescence imaging and fluorescence data also showed that Fv/Fm, Y (II), qN, qP, and Y (NPQ) were lower in the c3'h3 mutant than in the WT mutant, whereas Y (NO) was higher (Fig. 3a-l), indicating reduced photosynthetic efficiency in the c3'h3 mutant. Furthermore, the c3'h3 mutant had lower chlorophyll a, chlorophyll b, and carotenoid contents compared to the WT (Fig. 3m-o), and photosynthetic parameters of Pn (net photosynthetic rate), Gs (stomatal conductance), and Tr (transpiration rate) of the c3'h3 mutant were significantly lower than those of the WT (Fig. 3p-r). These results further indicated that the c3'h3 mutation reduces the photosynthetic efficiency of poplar.

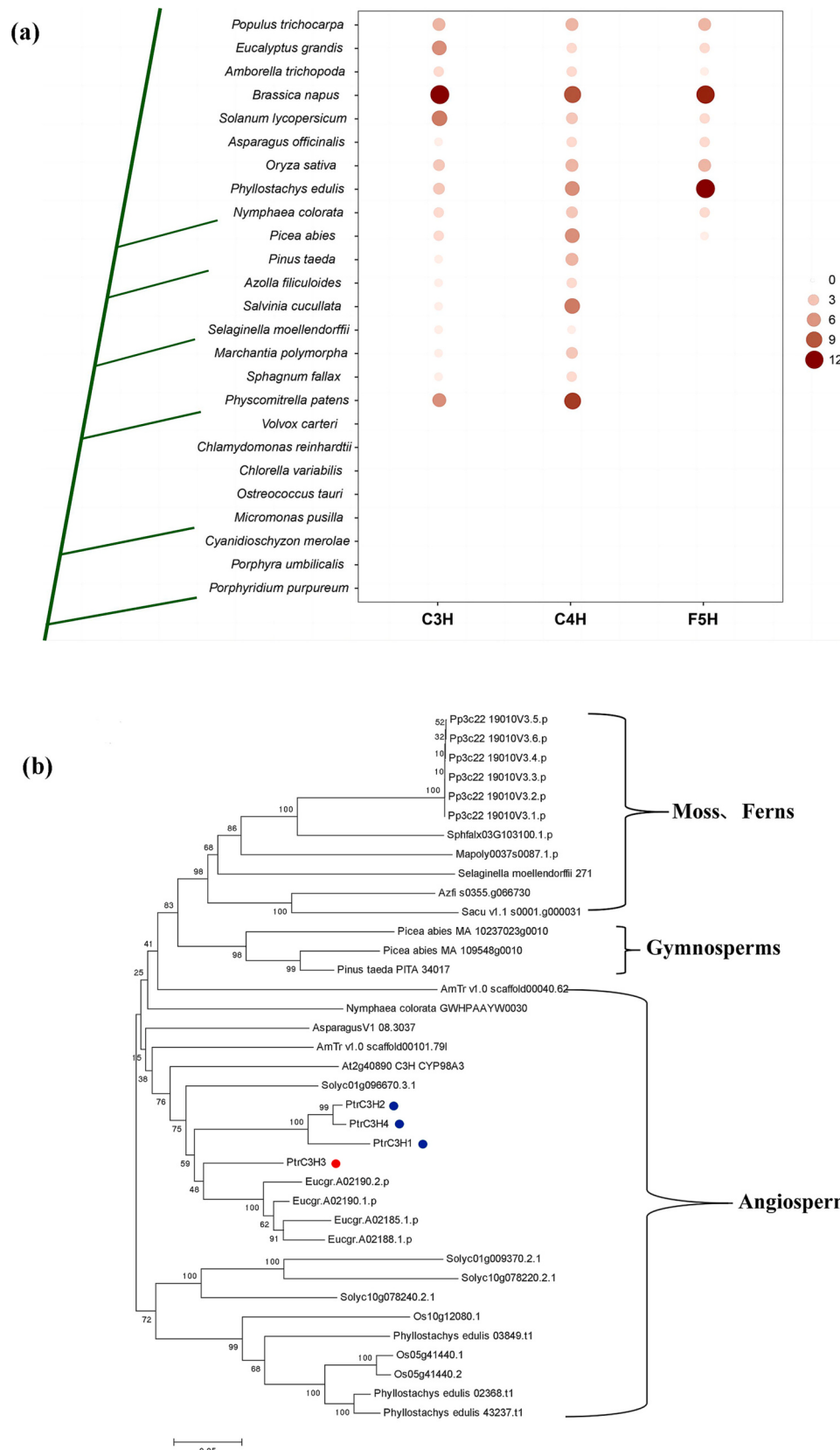


**Fig. 1.** Phylogenetic analysis of *C3'H* family and expression patterns of *C3'H* members in poplar.

(a) Phylogenetic tree analysis of the *C3'H* family. (b) Expression levels of the four *C3'H* genes in leaves, roots, apical, middle and basal parts of the stem, xylem, phloem and SAM (shoot apical meristem) in poplar. All data are means  $\pm$  SD ( $n = 3$ ).

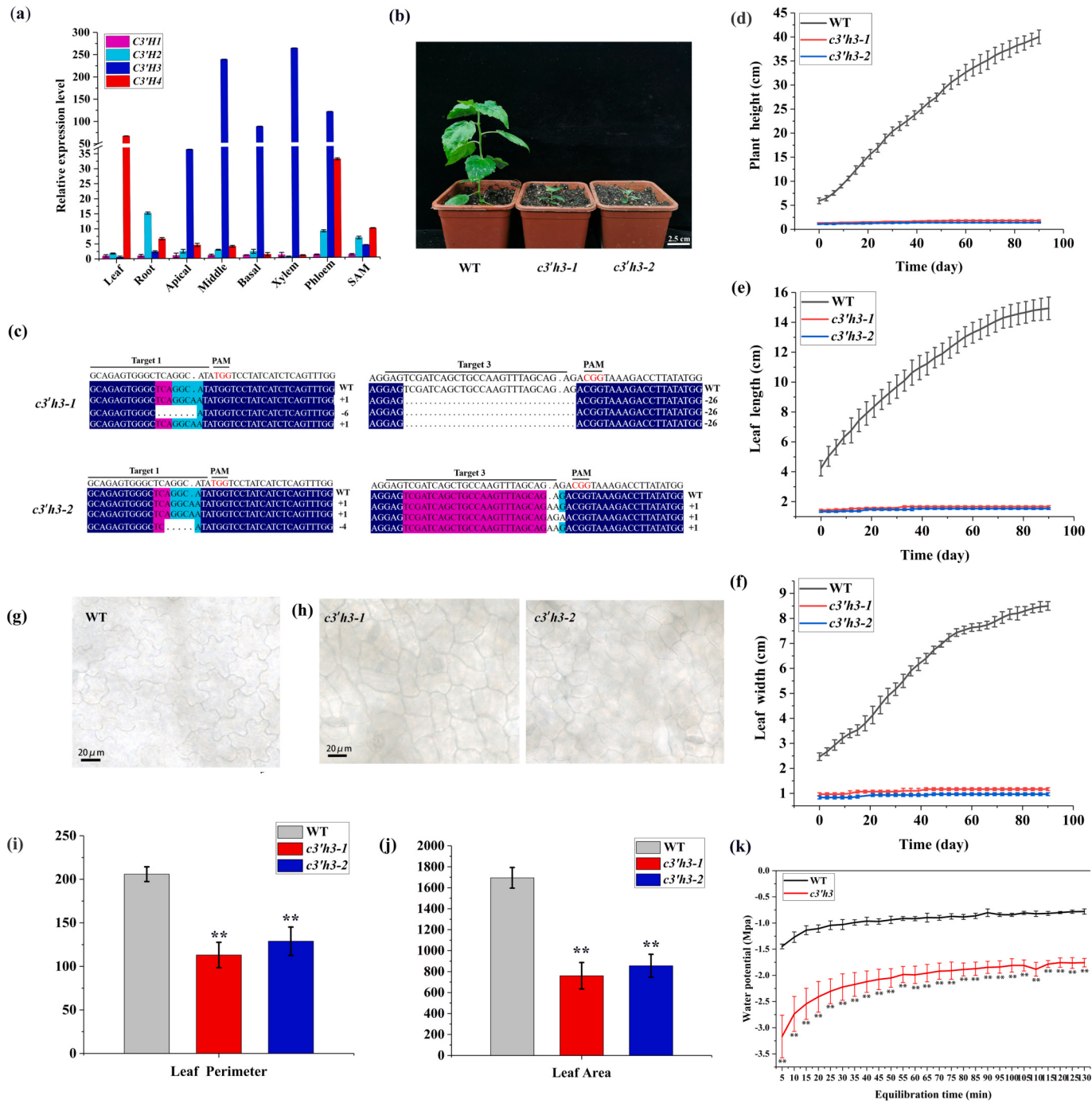


**Fig. 2.** *C3'H3* gene knockout by CRISPR/Cas9-mediated targeted mutagenesis in the transgenic poplar.

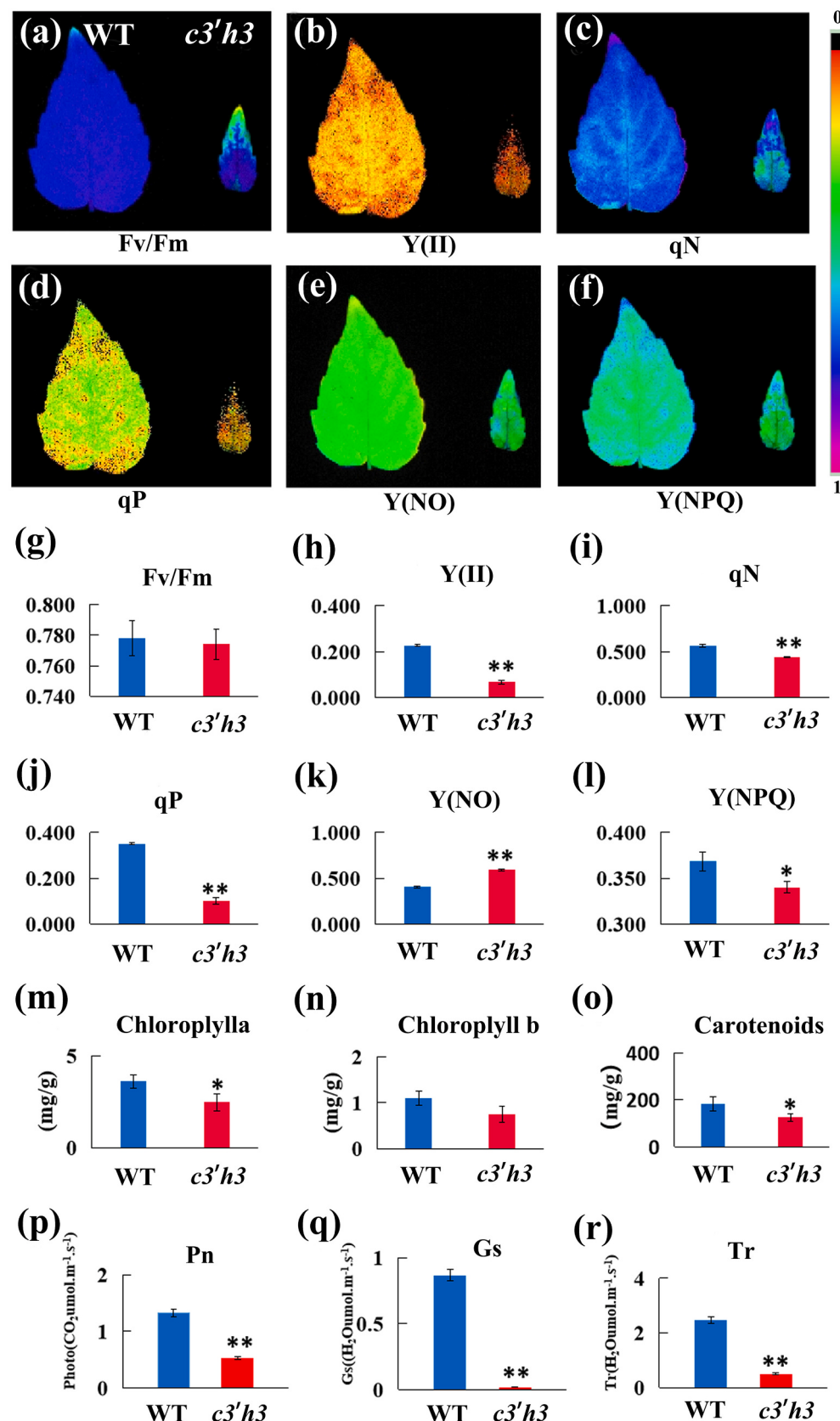
(a) Dwarf phenotypes of two *c3'h3* mutant plants. (b) Results of target sequencing. WT indicates no mutation in the chromosome, “-” indicates the deletion of the base in the chromosome, and “+” indicates the insertion of the base in the chromosome. (c) Plant height of WT and *c3'h3-1* and *c3'h3-2* mutants within 90 days. (d) Leaf length of WT and *c3'h3-1* and *c3'h3-2* mutants within 90 days. (e) Leaf width of WT and *c3'h3-1* and *c3'h3-2* mutants within 90 days. (f, g) Leaf cell observations of WT and *c3'h3-1* and *c3'h3-2* mutants. (h) Leaf perimeter of WT and *c3'h3-1* and *c3'h3-2* mutants. (i) Leaf area of WT and *c3'h3-1* and *c3'h3-2* mutants. (j) Water potential determination of WT and *c3'h3* mutants. All data are means  $\pm$  SD ( $n = 3$ ). Asterisks indicate significant differences between *c3'h3-1* and *c3'h3-2* mutants and WT plants based on Student's *t*-test (\* $p < 0.05$  and \*\* $p < 0.01$ ).

#### 2.4. The *c3'h3* mutant having irregular xylem and reducing lignin content

As mutations in lignin-related genes often produce irregular xylem [18], sections at the 3rd stem node and 2/3 of the main root were observed in the wild type and *c3'h3* mutant. The irregular xylem with collapsed vessels was only observed in the *c3'h3* mutant (Fig. 4 a-d), whereas thickened phloem cells were not observed in the 3-week-old stems of the *c3'h3* mutant. Secondary xylem was visible in the wild-

type root, and only weak protoxylem was observed in the *c3'h3* mutant (Fig. 4 e, f).

FT-IR spectra can indicate changes in chemical linkages [22–26], so an analysis of chemical structural changes between WT and *c3'h3* mutants was carried out. The peak intensity at  $1653\text{ cm}^{-1}$  (lignin aromatic C=C),  $1518\text{ cm}^{-1}$  (C=C and C—H bond in lignin aromatic ring),  $1250\text{ cm}^{-1}$  (C—O bond in the lignin),  $1155\text{ cm}^{-1}$  (coumarin structure of lignin), and  $830\text{ cm}^{-1}$  (S subunit lignin) in the *c3'h3* mutant was lower



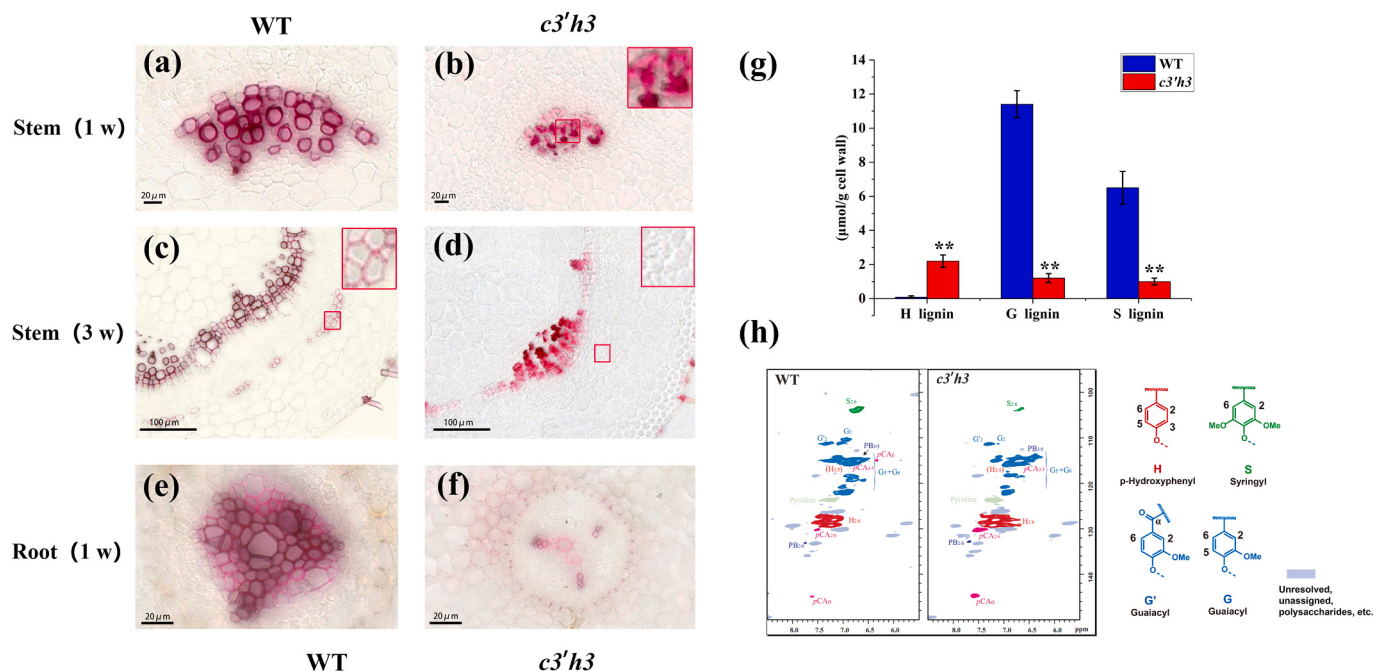


**Fig. 4.** Microscopic observation of section, leaf cell and lignin determination in WT and *c3'h3* mutants.

(a-d) The stem slices observations of WT and *c3'h3* mutants grown at 1- and 3-week-old, respectively. (e, f) Root slices observations of WT and *c3'h3* mutants grown at 1-week-old. (g) Water potential determination of WT and *c3'h3* mutants. (h) Lignin monomer content in WT and *c3'h3* mutants. (h) Aromatic regions of 2D <sup>13</sup>C-<sup>1</sup>H correlation (HSQC) spectra of cell wall gels from WT and *c3'h3* mutants in DMSO-*d*<sub>6</sub>/pyridine-*d*<sub>5</sub> (4:1) on the left, with the corresponding chemical formulae represented on the right to the different components on the left. The data show a decrease in S and G lignin and an increase in H lignin in the *c3'h3* mutant. All data are means  $\pm$  SD ( $n = 3$ ). Asterisks indicate significant differences between *c3'h3* mutant and WT plants based on Student's t-test (\* $p < 0.05$  and \*\* $p < 0.01$ ).

than that of the WT, indicating a decrease in lignin content in the *c3'h3* mutant compared to the WT (Fig. S2).

Thioacidolysis was used to measure the lignin monomer composition of the WT and *c3'h3* mutants. G- and S-lignin levels were significantly lower in the *c3'h3* mutant compared to the WT, but H-lignin levels were significantly higher (Fig. 4g). To determine the lignin differences between the *c3'h3* mutant and WT, both samples were collected and analyzed using the aromatic regions of 2D <sup>13</sup>C-<sup>1</sup>H correlation (HSQC) NMR spectra. The correlation between the S-subunit (S2/6) and the G-subunit (G2) was significantly lower in the *c3'h3* mutant, while the correlation of the H subunit was much stronger than that of the WT (Fig. 4h), which is consistent with thioacidolysis. Therefore, a decrease in G and S lignin and an increase in H lignin were observed in the *c3'h3* mutant.

Lignin defecton significant changes in the content of IAA and other endogenous hormones.

To explain the dwarf phenotype of the *c3'h3* mutant, endogenous hormones were measured at the apical, middle, and basal parts of the stem from the WT and *c3'h3* mutants. Although the IAA content in the apical part were less low in *c3'h3* mutant comparing with WT, the IAA contents in the middle and basal parts were significantly reduced in the *c3'h3* mutant compared to the WT (Fig. 5a), indicating auxin transport might be blocked in *c3'h3* mutant. Jasmonic acids (JAs) can induce stomatal opening as well as reduce transpiration and water loss [27–29]. The content of JA and JA-Ile (isoleucine conjugate) was significantly reduced in the *c3'h3* mutant compared to the WT (Fig. 5 b, c). However, the content of both SA and SA O-β-D-glucoside (SAG) was significantly increased in the *c3'h3* mutant (Fig. 5 d, e).

## 2.5. Changes in the expression of lignin-related genes

To figure out the genetic and metabolomic changes in the *c3'h3* mutant, six-week-old stems were collected for both transcriptomic and metabolomic analyses. 20 candidate genes were selected to verify the

RNA-seq data by RT-qPCR. The results show that the relative expression trends of the 20 genes are consistent with RNA-seq (Fig. S3), indicating the reliability of the transcriptome data. According to the KEGG database, differentially expressed genes (DEGs) were significantly enriched for phenylpropanoid biosynthesis (ko00940), phenylalanine metabolism (ko00360), flavonoid biosynthesis (ko00941), and plant hormone signal transduction (ko04075) (corrected q-value  $< 0.05$ , Fig. 6a). In the plant hormone signal transduction pathway, the expression levels of the early auxin response genes AUX/IAA (auxin/indole-3-acetic acid) and most SAURs (small auxin-up RNAs) were downregulated, whereas the negative regulator GH3 (Gretchen Hagen 3) was upregulated in the *c3'h3* mutant (Fig. 6b), consistent with the results for IAA content (Fig. 5a). In the phenylpropanoid biosynthesis pathway, the expression of C3'H upstream genes PAL, C4H, and 4CL was increased, whereas the expression of C3'H downstream genes CCoAOMT and F5H was declined in the *c3'h3* mutant (Fig. 6c). While the transcription levels of CHS, CHI, F3H, DFR, ANR, and LAR in the flavonoid biosynthesis pathway were upregulated in the *c3'h3* mutant. Additionally, four differentially expressed CADs were identified in the RNA-seq data, of which the three CADs raising in the *c3'h3* mutant may contribute to the enhanced H-lignin accumulation in the *c3'h3* mutant (Fig. 6c).

## 2.6. Lignin defecton enhanced flavonoid metabolic pathways

To better explain the flavonoid biosynthesis in the *c3'h3* mutant, metabolomic analysis was performed using HPLC-MS/MS. Both PCA and OPLS-DA analyses of the metabolomics data from the *c3'h3* mutant were clustered together and separated well from the WT lines (Fig. S4a, b). According to the volcano plot and KEGG enrichment analysis, most flavonoids were increased in the *c3'h3* mutant (Fig. S4c, d), consistent with the RNA-seq results. A total of 210 flavonoids were detected (Table S10). Among them, 66 flavonoids showed significant changes in the *c3'h3* mutant ( $VIP \geq 1$ ,  $|LogFC| \geq 2$ , Table S11). Out of these significantly changed flavonoids, 61 flavonoids were higher in *c3'h3*

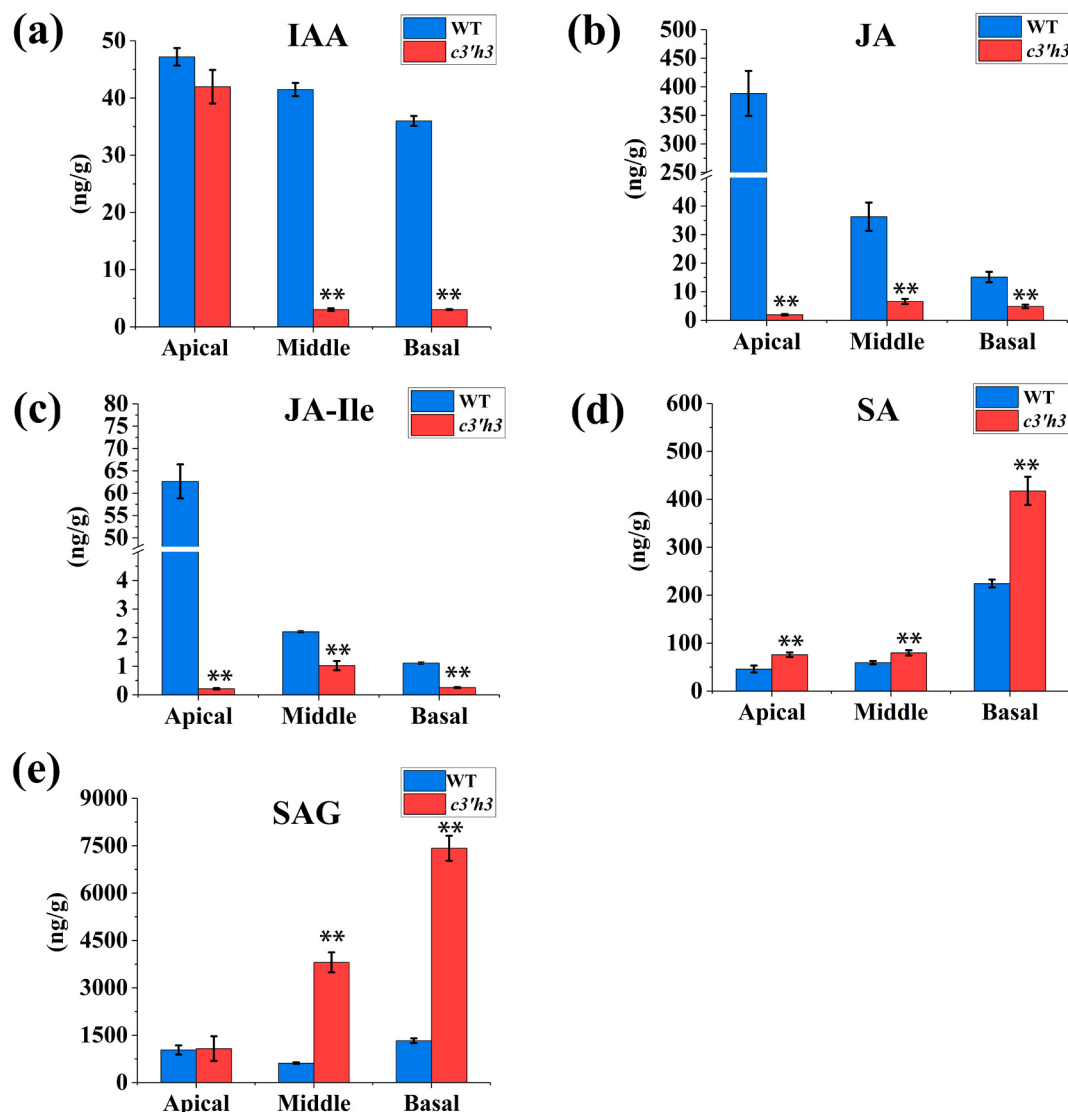


**Fig. 5.** Determination of endogenous hormone content in WT and *c3'h3* mutants.

(a-e): The content of endogenous hormone IAA, JA, JA-Ile, SA and SAG, respectively. All data are means  $\pm$  SD ( $n = 3$ ). Asterisks indicate significant differences between *c3'h3* mutants and WT plants based on Student's t-test ( $^*p < 0.05$  and  $^{**}p < 0.01$ ).

mutant lines than that in WT lines (Fig. 7a), confirming the enhancement of flavonoid metabolic flux after blocking the lignin metabolic flux in *P. tomentosa*.

In higher plants, the flavonoid biosynthesis pathway can be divided into three sub-fluxes by catalyzing naringenin with *F3'H*, *F3'5'H*, or FNSII sub-fluxes. Our results show that the top ten up-regulated flavonoids are mainly distributed in the *F3'H* and FNSII metabolic fluxes. Pelargonidin 3-O-beta-D-glucoside, fustin, and eriodictyol C-hexosyl-O-hexoside are synthesized through the *F3'H* metabolic flux. Vitexin 2'-O-beta-L-rhamnoside, 6-C-hexosyl luteolin O-pentoside, chrysanthemum O-malonylhexoside, tricin O-malonylhexoside, and luteolin O-hexoside O-feruloylpentoside belong to the FNSII metabolic fluxes (Fig. 7b). The most abundant significantly changed compounds are catechin, cyanidin 3-O-rutinoside, and procyanidin B3 (Fig. 7c). These metabolites are derived from naringenin via the *F3'H* metabolic flux. In addition, flavonoids in the FNSII metabolic flux, including chrysanthemum O-hexoside and chrysanthemum 5-O-glucoside, are also abundant in the *c3'h3* mutant. However, metabolites in the *F3'5'H* branching flux, such as dihydromyricetin, were not detectable in the extensive metabolomics analysis.

To further verify the flavonoid accumulation in the *c3'h3* mutant, we detected eight intermediate flavonoids in the branches of *F3'H*, *F3'5'H*,

or FNSII sub-fluxes using HPLC-QQQ-MS with commercial standards (Fig. 8a; Fig. S5). All eight flavonoids were found to be more abundant in the *c3'h3* mutant. In the *c3'h3* mutant, the levels of two substrates, naringenin chalcone and (S)-naringenin, increased to 117.07 and 34.51 ng/mg FW, respectively. Additionally, the content of luteolin in the FNSII metabolic flux increased by 4.41-fold. Moreover, the metabolic fluxes of *F3'H* showed an increase in (S)-eriodictyol, dihydroquercetin, and quercetin. Among them, (S)-eriodictyol increased 162.81-fold in the *c3'h3* mutant, which is consistent with the extensive metabolomic data (Fig. 8b; Fig. 7). In contrast to the metabolomics data, dihydromyricetin in the *F3'5'H* metabolic flux was detected in the *c3'h3* mutant using HPLC-QQQ-MS. Furthermore, the metabolomics data showed a 31.89-fold increase in hesperetin content (Fig. 8a). Interestingly, after treated with hesperetin, epidermal root cells of *Arabidopsis* were reduced the number and length of cells in the root meristem tissue (Fig. 8c), suggesting that the accumulation of secondary flavonoid metabolites may inhibit cell division and cell growth.

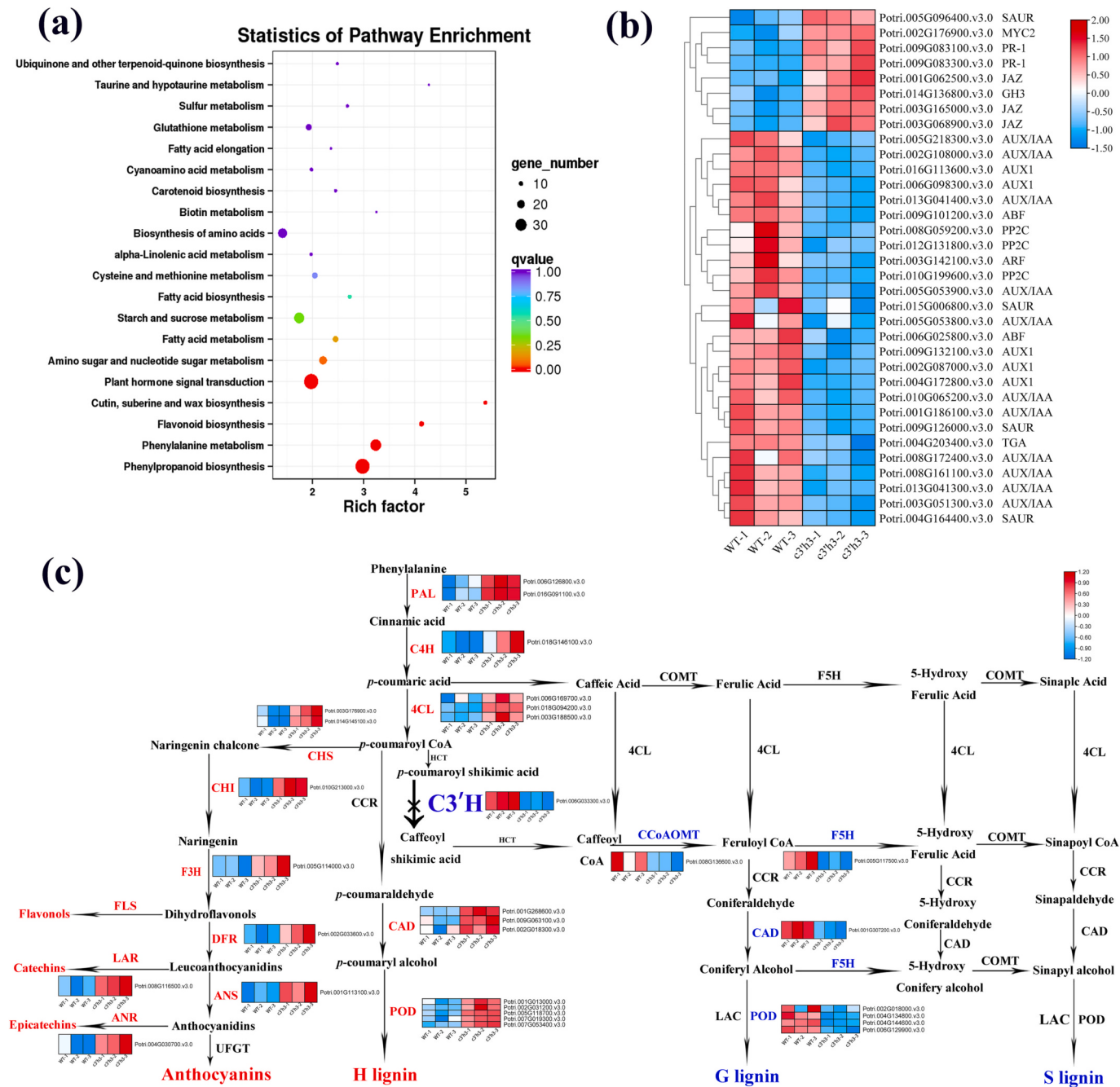


**Fig. 6.** KEGG enrichment and differentially expressed genes in the biosynthesis of phenylpropanoids in the *c3'h3* mutant.

(a) KEGG enrichment of WT and *c3'h3* mutants. (b) Differentially expressed genes in plant hormone signal transduction pathway in the *c3'h3* mutant. (c) Differential genes differ in the phenylpropanoid biosynthesis pathway and branch into the lignin biosynthesis and flavonoid biosynthesis pathways.

### 3. Discussion

#### 3.1. Lignin evolution in plants

Land plants evolved from freshwater green algae about 480 million years ago [30]. Lignin evolved concomitantly with the rise of vascular plants on Earth 450 million years ago [31]. Fossil evidence and phylogenetic studies showed that the earliest land plants were small in stature and simple in morphology, similar to bryophytes (moss, etc.) that exist today [32]. With the evolution of vascular plants, the establishment of diverse new protective mechanisms was required to overcome new or elevated stresses such as UV irradiation, drought, rapid temperature fluctuations, and gravity [33]. Therefore, upright plants need

biosynthesize lignin to provide mechanical support in secondary cell walls, promoting vascular plants to tall heights and facilitating long-distance water transport [34,35]. Phenylpropanoid-derived natural products were probably driving forces during land plant evolution [12]. Lignin is a class of 4-hydroxyphenylpropanoid-derived biopolymers uniquely and ubiquitously associated with vascular plants [36]. Except for S lignin, which is restricted to some lineages such as flowering plants, Selaginellaceae, and some species of ferns and gymnosperms, H and G lignins are present in all vascular plants [12,31].

Lignin is a complex three-dimensional, branched heteropolymer of bonded hydroxycinnamyl alcohols that crosslink carbohydrate polymers together, thereby rigidifying plant cell walls [16]. In the monolignol pathway, the *C3H*, *C4H*, and *F5H* cytochrome P450 monooxygenases

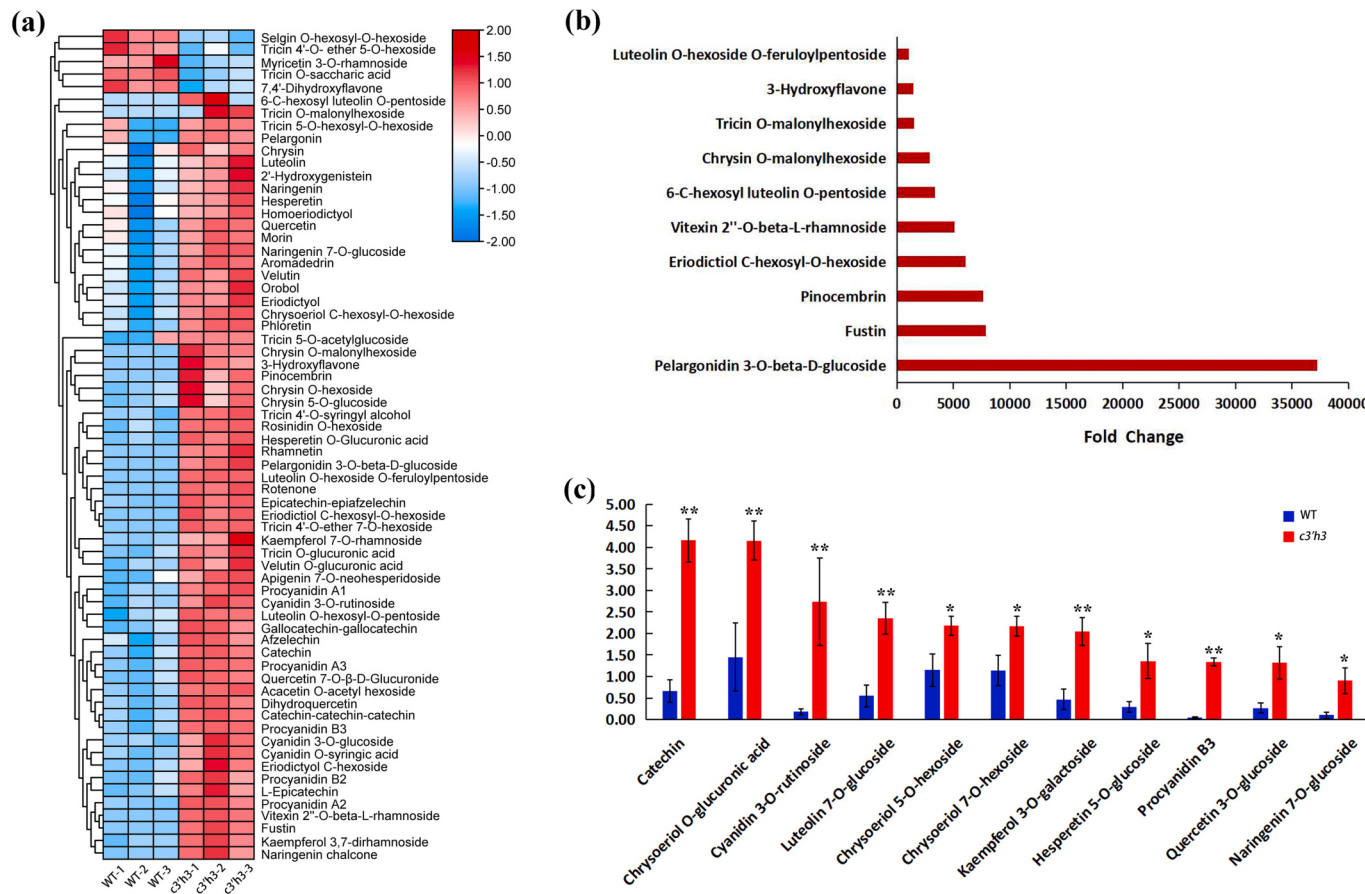


**Fig. 7.** Significant changes in flavonoids in the *c3'h3* mutant.

(a) Heat map of significant changes in flavonoids in the *c3'h3* mutant. Red colour indicates increased accumulation and green colour indicates decreased flavonoids in the *c3'h3* mutant. (b) Top 10 up-regulated flavonoids among the highly accumulated up-regulated flavonoids in the *c3'h3* mutant; (c) Most abundant flavonoids among the highly accumulated up-regulated flavonoids in the *c3'h3* mutant. Asterisks indicate significant differences between *c3'h3* mutants and WT plants based on Student's t-test (\* $p < 0.05$  and \*\* $p < 0.01$ ).

catalyze, respectively, the three, four, and five hydroxylation of monolignol precursors [37]. Phylogenetic analysis of the 275-member cytochrome P450 superfamily in *Arabidopsis* suggests that *C3H* and *C4H* evolved from a common ancestor, which led to the identification of CYP98A3 as the *C3H* gene in *Arabidopsis* [38]. However, *F5H* was more distantly related to *C4H* and *C3H* cytochrome P450 monooxygenases and had been identified in only a few eudicot species and not in gymnosperms, consistent with its role in S lignin synthesis [38,39] and also consistent with our results (Fig. S1; Fig. 1a). A previous study showed that moss was a basal lineage of land plants and a key evolutionary point for vascular development, which is consistent with our result that there are no *C4H* and *C3H* genes before moss for evolution (Fig. 1a). The *C4H* gene progenitor appears to have duplicated in early seed plants, resulting in two clades that are preserved in Taxaceae and most angiosperms. Furthermore, a second duplication event happened after the divergence of dicots and monocots [40].

Coumarate 3-hydroxylase and *C3'H* catalyze the conversion of p-coumarate and p-coumaroyl shikimate into caffeate and caffeoyl shikimate (via a cytochrome P450 monooxygenase) [38], respectively. These enzymes play important roles in G-lignin and S-lignin biosynthesis [40]. CYP98 in moss uses p-coumaroyl-threonate as a substrate, whereas *C3'H* in higher plants uses p-coumaroyl shikimate as a substrate, which leads to the distinct biosynthetic pathway for cuticle [38,41]. *C3H* orthologs are present in all land plants [31], often as single-copy genes, and their emergence preceded the occurrence of lignin.

In our study, the number of *C3H* homologs detected in 25 plant species shows that no *C3H* genes in green and red algae, which grow in a

very humid environment. There are a few *C3H* genes in mosses, ferns, and gymnosperms, and more genes emerge in angiosperms during land plant evolution (Fig. 1a). Furthermore, we performed phylogenetic analysis of *C3'H* among different species, and the results show that they are classified into three groups: mosses and ferns, gymnosperms, and angiosperms. There were four *C3'H* homologous genes (*PtrC3'H1*, *PtrC3'H2*, *PtrC3'H3*, and *PtrC3'H4*) in poplar with close genetic distance (Fig. 1b). Additionally, *PtrC3'H3* was recognized as the homolog of *Arabidopsis C3'H* [40], which is consistent with our results (Fig. 1b).

### 3.2. Optimized CRISPR/Cas9 system can efficiently study lignin deflection

Previous reports of *C3'H* in wood have mainly been studied using RNA interference (RNAi) [42,43]. This approach only results in the downregulation of target genes or simultaneous silencing of closely related homologous genes [44]. CRISPR/Cas9 gene editing technology is an effective tool for targeting and knocking out specific genes [44,45]. Our *c3'h3* mutant exhibits a more severe phenotype compared to the RNAi approach, which can help us gain a better understanding of the function of lignin in poplar.

As an efficient genome editing technology, the CRISPR/Cas9 system has been successfully applied to a wide range of plant species [46]. The gene editing efficiency varies among plant species due to different genome structures, such as GC content and genome size. Furthermore, high transformation efficiencies have been reported in monocot species, such as maize (57 %), wheat (80 %), and rice (64 %) [47]. However, there are still many unclear problems for application in dicots, especially

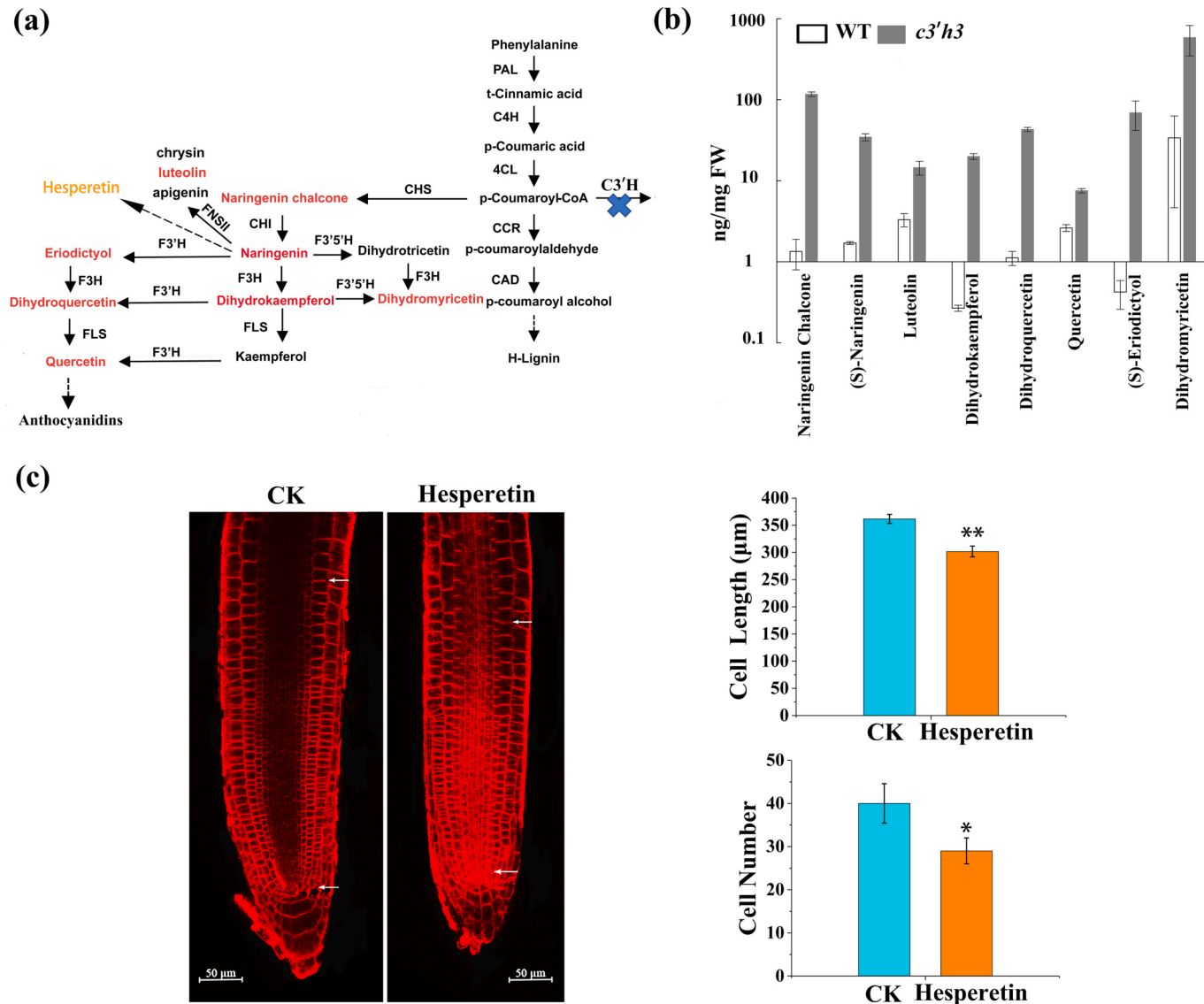


**Fig. 8.** High accumulation of up-regulated flavonoids and flavonoids detected in the *c3'h3* mutant.

(a) Flavonoid metabolism pathway; red represents the detected flavonoids, orange represents hesperetin. (b) Flavonoids detected by HPLC-QQQ-MS in *c3'h3* mutant. (c) Observation of root meristem cells of *Arabidopsis* after hesperetin treatment.

in woody plants [48], such as the efficiency caused by the number of targeting sites and single-target multi-gene vectors in woody plants. Therefore, optimization of the CRISPR/Cas9 system is required to enable its effective application in different species [49]. Currently, the main approach to increase mutation rates in the CRISPR/Cas9 system is to increase Cas9 or gRNA expression [50]. For example, using different constitutive, tissue- or germline-specific promoters to drive the expression of Cas9 has been demonstrated in plants [51,52].

In this study, the cleavage of the poplar genome could not be well guided by CRISPR/Cas9 system by a single-site construct. In contrast, a targeting vector with three sites of the *C3'H3* gene could produce the positive mutation homozygotes. Although the Cas9 vector with a single target site was much more efficient in targeting herbaceous rice, for woody plants, we recommend using 2–3 target sites for a single gene to improve targeting efficiency as previous report [53].

### 3.3. Lignin deflection resulted in dwarf phenotype and affected water transport in *Populus tomentosa*

Lignin is the main product of this pathway with important biological

functions that play a significant role in enhancing the mechanical strength and hydrophobicity of tracheary elements [54]. Some studies have suggested that dwarfism in phenylpropanoid-deficient mutants, such as *ref8*, is caused by the effect of lignin deficiency-induced vascular collapse and structural changes on water transport [54–57]. The hydraulic conductivity of the downregulated *C3'H* lines in poplar was significantly reduced by approximately 34 % during the same growth stage compared to the WT [58,59]. *C3'H*-knockout mutants generated in rice were severely dwarfed and sterile [56]. Similarly, in our study, *c3'h3* mutants also exhibited a severe dwarf phenotype, with significantly lower leaf length, width, plant height, and cell size compared to those of the WT (Fig. 2c-i). These traits indicate that the knockout of *C3'H3* affects normal growth and development in *Populus tomentosa*.

The plant cell wall provides mechanical support to the plant cell and participates in biotic and abiotic stress responses [2]. The disruption of the cell wall enzymes often has significant consequences on plant growth and development [60]. In *Arabidopsis*, the *lew2* mutant, which has an AtCesA8 defect, exhibits collapsed xylem cells and obstructed water transport, resulting in wilting. Xylem vessels are key factors related to mechanical support and water transport in plants [37,61]. In

our study, the knockout of *C3'H3* led to the formation of irregular xylem with collapsed vessels (Fig. 4 a-d). Additionally, xylem tension exists because the water column is engaged in a ‘tug-of-war’ between adhesion to soil particles and evaporation from the leaf surface. This tension can also be described as ‘negative pressure,’ quantitatively referred to as water potential. Increasingly negative water potentials indicate greater tension imposed on the water column [62]. Our results show that leaf water potential was significantly reduced in the *c3'h3* mutant (Fig. 2j). This indicates that the collapsed xylem of the stem will decrease water potential. As a result, the *c3'h3* mutant exhibited reduced water uptake from roots, inhibited growth, and ultimately died (Data S1). Previous studies have also suggested that the ancestral function of G lignin is associated with reinforcing the cell wall of water-conducting tracheary elements [31,37]. Additionally, the water-conducting cells in both gymnosperms and angiosperms primarily comprise G lignin, suggesting a strong selective pressure to conserve the pathway of G lignin biosynthesis in the water-conducting cells of xylem during land plant evolution [37]. In our study, the G lignin content significantly decreased in the *c3'h3* mutant, suggesting weakened water conductivity. Therefore, *C3'H3* may play an important role not only in regulating plant growth but also in transporting water.

#### 3.4. Lignin defect reduced photosynthetic efficiency and auxin content

Plants use photosynthesis to convert carbon dioxide and water into energy-storing organic sugars and release oxygen, which is then converted into carbohydrates and eventually stored in lignocellulose [63]. In our study, Y (II), qN, qP, and Y (NPQ), as well as other PSII parameters such as Y (NA), ETR (II), NPQ, and qL, were significantly reduced in the *c3'h3* mutant compared to WT (Fig. 3; Table S1). This implies a reduced photosynthetic rate in the *c3'h3* mutant as others [64–70]. The chlorophyll content of leaves is another important factor in determining photosynthetic efficiency and plant growth, which is directly related to the Pn intensity of plants [71]. Chlorophyll content and photosynthetic rate decrease due to water deficiency in soybeans, resulting in a decrease in plant height [72]. In our study, both the net photosynthetic rate and chlorophyll content of *c3'h3* mutants were also significantly lower than WT (Fig. 3m-p). Phloem plays important roles in metabolomic transport [18], which is consistent with our results showing the disappearance of secondary phloem in the *c3'h3* mutant (Fig. 4 a-d). The disappearance of phloem in the *c3'h3* mutant may also provide feedback to limit photosynthesis.

Endogenous plant hormones regulate plant growth [73]. Auxin is an important hormone that promotes the growth and development of plant cells, organs, and tissues, as well as regulates apical dominance and tropism [74]. Auxin can be transported from the apical synthesis site to other organs of the plant, where it affects plant growth and development and participates in many physiological processes, such as lateral root formation, root, and leaf growth and development [75–77]. In our study, IAA content was significantly reduced in the middle and basal parts of the *c3'h3* mutant (Fig. 5a), indicating blocked auxin transport in the *c3'h3* mutant, which is consistent with the *c3'h3* mutant lacking obvious phloem thickening. Additionally, *AUX1* (Auxin influx carrier) genes, which are positive regulators of the auxin signal transduction pathway, were down-regulated in the *c3'h3* mutant, whereas *GH3* (Gretchen Hagen 3) genes, which are negative regulators of the auxin pathway [78,79], were up-regulated in the *c3'h3* mutant (Fig. 6b). Therefore, we deduce that the knockout of *C3'H3* decreased the transport of auxin, thereby limiting plant growth.

In addition, salicylic acid (SA) is considered an important compound for signal transduction in plant defense responses against damage caused by abiotic and biotic stresses [80]. Furthermore, excessive accumulation of SA metabolites in some transgenic plants often leads to a dwarf phenotype [81,82]. However, reducing SA levels or enhancing its degradation through genetic engineering can alleviate dwarfism in HCT-RNAi plants [83]. On the other hand, preventing SA accumulation

in the *ref8-1* mutant did not restore growth [84]. In our study, SA content was significantly increased in the *c3'h3* mutant (Fig. 5d). However, the relationship between SA content and growth in the *c3'h3* mutant needs to be further discussed.

#### 3.5. Lignin defect resulted in significant increase in flavonoid content

Transcriptomic and metabolomic analyses were performed to identify genetic and metabolomic changes in the *c3'h3* mutant and further dissect the underlying molecular causes of the dwarf phenotype. The flavonoid biosynthetic metabolic pathways showed significant enrichment, and the *c3'h3* mutant plants exhibited increased expression of the most significant genes associated with secondary metabolism (Fig. 6a, Table S2). Secondary metabolism appeared to be balanced at *p*-Coumaroyl-CoA. The upstream genes *PAL*, *C4H*, and *4CL* were upregulated, while the downstream genes *CCoAOMT* and *F5H* were downregulated in the *c3'h3* mutant. This resulted in the blockage of G and S lignin synthesis, but the H lignin synthesis and flavonoid biosynthesis pathways were activated. Additionally, the genes *CHS*, *CHI*, *F3H*, *DFR*, *ANS*, *FLS*, *LAR*, and *ANR* were upregulated (Fig. 6c). The GO term analysis revealed that the majority of down-regulated genes were related to basic processes of growth and development in these plants (Table S3). Furthermore, metabolome analysis indicated that the flux of flavonoid metabolism was enhanced after blocking the lignin metabolic flux by knocking out the *C3'H3* gene in *P. tomentosa* (Fig. 7a). Previous research has also demonstrated that restriction of the lignin pathway leads to metabolic flux redirection toward the interconnected flavonoid branch, resulting in the excessive accumulation of flavonoids [85,86]. Interestingly, studies have shown that flavonoids such as naringenin, quercetin, and kaempferol act as auxin transport inhibitors, and the excessive accumulation of endogenous flavonoids can affect auxin transport in mutants [87,88]. In our study, the *c3'h3* mutant exhibited an 8.76-fold increase in naringenin, a 6.82-fold increase in quercetin, and a 7.09-fold increase in kaempferol (Table S10), so it is possible one of the reasons of blocking auxin transport.

Based on our results, we propose a working model to explain the reasons for limiting the growth and resulting in the dwarf phenotype in *C3'H3* mutants (Fig. 9). *C3'H* plays an important role in lignin biosynthesis. There are four *C3'H* genes (*PtrC3'H1*, *PtrC3'H2*, *PtrC3'H3*, and *PtrC3'H4*) in *Populus trichocarpa* (Fig. 1b), with *PtrC3'H3* being highly expressed in the xylem, phloem, apical, middle, and basal parts of the stem compared to the other three *C3'H* genes (Fig. 2a). After knocking out *C3'H3*, irregular xylem with collapsed vessels was only observed in the *c3'h3* mutant. The water potential in *c3'h3* mutant plants was reduced due to irregular xylem vessels. Simultaneously, auxin transport was reduced due to the lack of phloem thickening. Additionally, flavonoid metabolites such as naringenin and hesperetin were considerably accumulated. Thus, we can deduce that the lignin defect suppressed plant growth and caused the dwarf phenotype through collapsed xylem and phloem thickening, limiting material exchanges and transport.

## 4. Materials and methods

### 4.1. Plant materials and growth condition

Plant materials and growth conditions: *P. tomentosa* tissue culture seedlings were obtained from the Chinese Academy of Forestry Sciences (Beijing, China). Wild-type and transgenic plants were grown in a thermostatic seedling culture room ( $25 \pm 1^\circ\text{C}$ , with a light duration and light intensity of  $16 \text{ h.d}^{-1}$  and of  $35 \mu\text{mol}\cdot\text{m}^{-2}\cdot\text{s}^{-1}$ , respectively).

### 4.2. Plasmid vectors

Vectors: The dicotyledonous Cas9 protein plasmid vector (pYL-CRISPR/Cas9-DN) and sgRNA vectors (pYLgRNA-AtU3d/LacZ, pYLgRNA-AtU6-1, and pYLgRNA-AtU6-29) were obtained from the

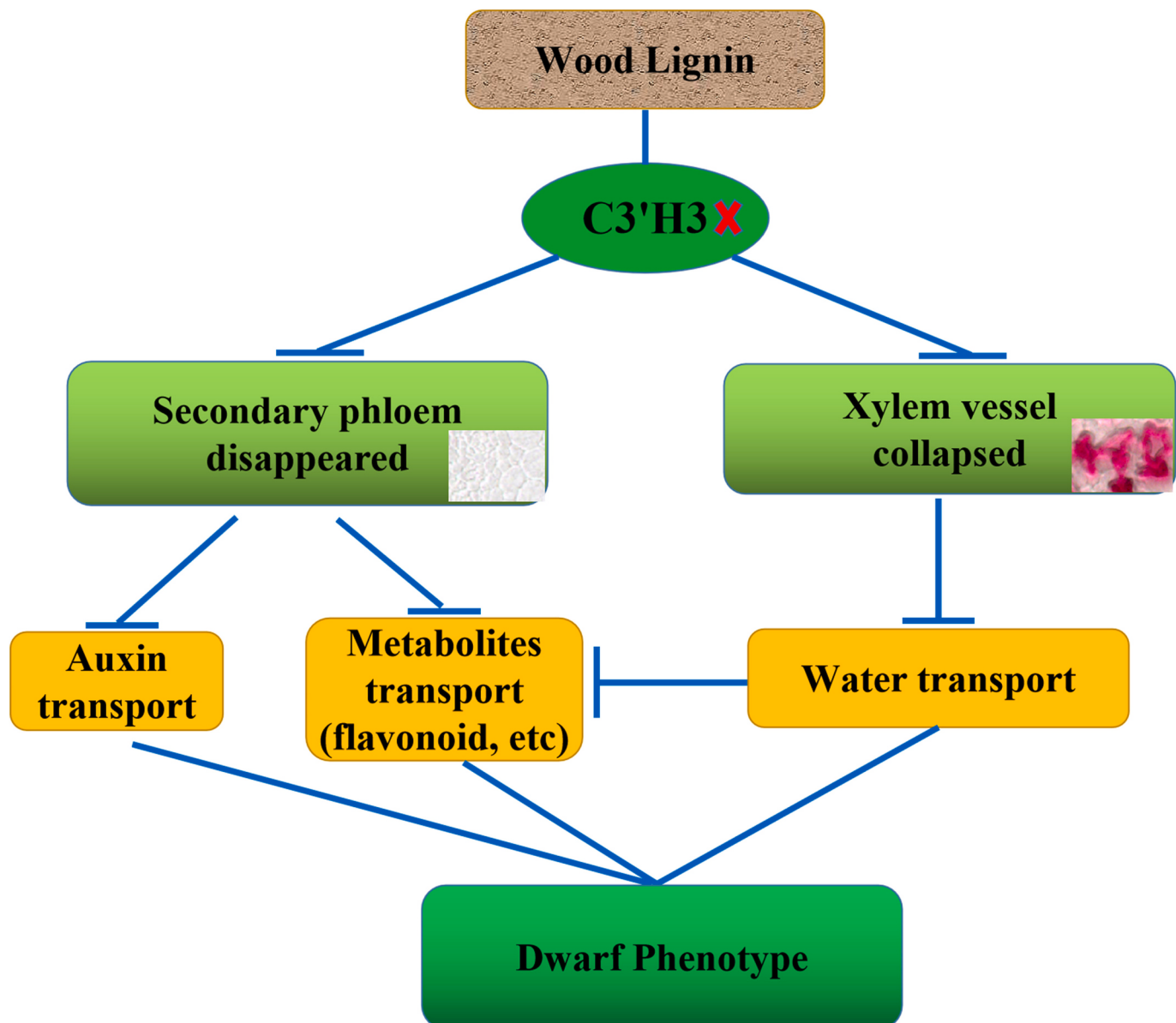


**Fig. 9.** A working model to restrict the cause of growth and result in dwarf phenotype in *c3'h3* mutants.  
The red fork in oval indicates the removal of *C3H3* gene; The blue vertical line together with horizontal line indicate inhibition.

research group of Professor Yaoguang Liu at South China Agricultural University.

#### 4.3. Phylogenetic analysis

A phylogenetic tree was constructed using the neighbor-joining (NJ) method, and 1000 bootstrap replicates were performed using MEGA 7.0. Alignments used to generate the phylogenies are shown in Data S2.

#### 4.4. Expression level analysis of *C3'H* genes

To verify the expression levels of four homologous genes *C3'H1*, *C3'H2*, *C3'H3*, and *C3'H4* in different tissues, eight tissues were sampled: xylem, phloem, apical, middle, and basal regions of the stem, root, leaf, and shoot apical meristem (SAM). Sequences were obtained from [http://genome.jgi-psf.org/Poptr1\\_1/](http://genome.jgi-psf.org/Poptr1_1/) (Table S4), and RT-qPCR primers were designed using Primer 5.0 (Table S5).

#### 4.5. RNA extraction

Total RNA was extracted from the apical, middle, and basal parts of the stem, leaf, root, xylem, phloem, and shoot apical meristem (SAM) using the RNAPrep Pure Plant Plus kit (TIANGEN, Beijing, China) following the manufacturer's instructions. The concentration of RNA was determined using a NanoPhotometer® spectrophotometer (IMPLEN, CA, USA), and the quality and integrity of the RNA were assessed using a 1% agarose gel and the RNA Nano 6000 Assay Kit with the Bioanalyzer 2100 system (Agilent Technologies, CA, USA).

#### 4.6. RT-qPCR analysis

cDNA was synthesized using the PrimeScript™ RT reagent Kit with gDNA Eraser (Perfect Real Time) (Takara, Dalian, China). The synthesized cDNA was then diluted 10-fold and used as a template for RT-qPCR. The RT-qPCR reactions were performed using the SYBR® Premix Ex Taq II (Tli RNase Plus) (Takara, Dalian, China) according to the instructions on a LightCycler 480 instrument (Roche Molecular

Biochemicals, Mannheim, Germany). Actin was used as the reference gene for RT-qPCR in *P. tomentosa* [89], and the primers for RT-qPCR are listed in Table S6. Three biological replicates were used for each reaction, and the relative expression level of each gene was calculated using the  $2^{-\Delta\Delta CT}$  method [90].

#### 4.7. Construction of vectors

The vectors pYLCRISPR/Cas9-DN and CRISPR/gRNA were obtained from Liu's lab, and their protocols were described by Ma et al. [91]. To enhance the mutation efficiency of the *C3'H3* gene, three target sites were designed. Target sites were located at the functional domain of the ORF. Mutations in any of the target sites could potentially result in loss of function. Among the three target site vectors constructed, the gRNA promoter for T1 was Atu3d, the gRNA promoter for T2 was Atu6-1, and the gRNA promoter for T3 was Atu6-29. The primers for each target site are listed in Table S7. The primer sequences for the gRNA expression cassettes, required for both rounds of PCR, are shown in Table S8. Positive clones were confirmed by sequencing the specific target site using the corresponding primer, following the method described by Ma et al. [91]. After successful sequencing, the pGWB101 vector [92] was recombined and transferred into Agrobacterium competent cell LBA4404. The colonies were then identified by PCR for *P. tomentosa* transformation.

#### 4.8. Genetic transformation of *Populus tomentosa*

The genetic transformation was conducted using the Agrobacterium-mediated leaf disk method to infect the leaves of *P. tomentosa*, following the protocol described by Li et al. [93]. To identify *c3'h3* mutants, the sgRNA target sequence was incorporated into the flanking primers for PCR amplification. The resulting PCR products were ligated into the T-vector, and at least 20 colonies were selected for sequencing. The primer sequences can be found in Table S9.

#### 4.9. Measurement of growth parameters

After one week of acclimatization, the plant height (from the plant soil surface to the top bud) and leaf length and width (measured with vernier calipers) of both WT and *c3'h3* mutants were measured to track changes in the *c3'h3* mutants over a period of 90 consecutive days. Once stable growth was achieved for both WT and *c3'h3* mutants (approximately 1 month after transplanting into the soil), the leaves were treated with 95 % alcohol for one week to remove chlorophyll. Subsequently, the leaf cells were observed, and an automatic digital scanning imaging system (Wanbang Junyi M8, Beijing, China) was used for further determination of leaf perimeter and area.

#### 4.10. Chlorophyll fluorescence and Chlorophyll content assay

The chlorophyll fluorescence of leaves in both the WT and *c3'h3* mutants was assayed using the Maxi Imaging-PAM M-series (Heinz Walz GmbH, Germany). The Pn, Gs, and Tr of leaves in the WT and *c3'h3* mutants were measured using the portable photosynthetic analyzer Licor-6400 (Licor, Lincoln, NE, USA), following the method described by Timm et al. [94]. Several parameters related to photosynthesis, including PSI-containing ETR (I), Y (I), Y (ND), Y (NA), and PSII-containing ETR (II), Y (II), qN, qP, Y (NO), Y (NPQ), NPQ, qL, and Fv/Fm, were measured to evaluate photosynthetic efficiency (Table S1). The assays were performed with three biological replicates.

Fresh leaves weighing 0.5 g from both the WT and *c3'h3* mutants were soaked in 5 mL of 95 % ethanol and kept in the dark for 1 week to obtain a mixed solution, referred to as the extract. The chlorophyll content was then assayed as follows: the absorbance values of the extracts at wavelengths of 470 nm, 649 nm, and 665 nm were recorded, and the chlorophyll content was calculated according to the method

described by Dai et al. [95]. All measurements were performed three times.

#### 4.11. Observation on the lignification of stems and roots

The 3rd stem node (counted from apical to basal) and roots of 1- and 3-week-old seedlings from both the WT and *c3'h3* mutants were embedded in 3 % agarose (Biowest, BY-R0100, Spain) by mass/volume ratio. The stems were cut into 40  $\mu$ m thickness, and the roots were cut into 50  $\mu$ m thickness using a vibratome (Leica VT1000S, Microsystems, USA). The sections were then placed on slides and stained with 3 % phloroglucinol for 5 s, followed by washing off the stain with concentrated HCl (37 M). The slices were observed and photographed using an automatic digital scanning imaging system (Wanbang Junyi M8, Beijing).

After achieving stable growth of the WT and *c3'h3* mutants (approximately 1 month after transplantation into the soil), the water potential was measured using a dew-point water potential instrument (Psypyro, USA) following the manufacturer's instructions.

#### 4.12. Determination of endogenous hormone content

The apical, middle, and basal parts of the stem from both the WT and *c3'h3* mutants were taken and ground into powder using liquid nitrogen. Approximately 100 mg of the powder was weighed into a centrifuge tube and then placed in dry ice before being transported to Zhejiang Normal University for hormone determination.

#### 4.13. Fourier transform infrared spectroscopy analysis (FT-IR)

FT-IR spectra were obtained following the procedure described in the relevant literature [24]. Dried samples of 1 mg from both the WT and *c3'h3* mutant were mixed with 100 mg of KBr and ground into particles with a diameter of 2 mm. The resulting mixture was used to prepare KBr supplemental tablets and analyzed using a spectrophotometer as described by Zhu et al. [24], with a wavelength scanning range of 2000–400  $\text{cm}^{-1}$ , a resolution of 4  $\text{cm}^{-1}$ , and 32 scan times.

#### 4.14. Determination of lignin content

To determine the lignin content in both the WT and *c3'h3* mutants, 300 mg of poplar powder (40–60 mesh) was hydrolyzed using 3 mL of 72 % H<sub>2</sub>SO<sub>4</sub> at 32 °C for 1 h, resulting in a mixture. Subsequently, 84 mL of deionized water was added to the mixture, which was then maintained at 121 °C for 1 h to facilitate further hydrolysis. Finally, the hydrolyzed mixture was filtered through a G4 sand core funnel. The change in mass before and after filtration was measured to obtain the lignin content [96].

#### 4.15. <sup>13</sup>C NMR and 2D-HSQC spectra

WT and *c3'h3* mutant lignin samples were obtained using a 600 MHz Bruker Avance instrument, following the procedure described by Zhu et al. [24]. For <sup>13</sup>C NMR analysis, reference to Zhu was made. Specifically, 60 mg of lignin was dissolved in 0.5 mL of DMSO-*d*<sub>6</sub> (deuterated dimethyl sulfoxide) for 2D-HSQC (2D heteronuclear single-quantum coherence) analysis. The sampling time was 0.17 s, the relaxation time was 1.5 s, sampling was done 128 times, and the scanning time was 6 h, as described by He et al. [97].

#### 4.16. FM4-64 staining

FM4-64 staining of Arabidopsis epidermal root cells treated with hesperetin was conducted following the methods described by Rigal et al. [98]. Additionally, to observe cellular changes after hesperetin treatment, the number of cells and cell length were determined.

#### 4.17. RNA-seq

Stems of 1-month-old WT and *c3'h3* mutants were selected for RNA-seq analysis. Two groups of samples were prepared with three biological replicates each. The analysis was outsourced to BioMarker (Beijing, China). Differential expression analysis of WT and *c3'h3* mutants was conducted using the DESeq R package (version 1.10.1). Genes with  $|\log_2(\text{fold change})| \geq 1$  and a *P*-value  $< 0.05$ , as determined by DESeq, were considered differentially expressed. Functional enrichment analysis of the differentially expressed genes (DEGs) was performed using the KEGG database, with a threshold q-value  $< 0.05$ . The DEG results were visualized as heatmaps based on FPKM values using TBtools software. The RNA-seq data were submitted to <http://bigd.big.ac.cn/gsa/> with submission number: CRA007139.

#### 4.18. Metabolomic analysis

The materials used were the same as those used for RNA-seq analysis, which was outsourced to MetWare (Wuhan, China). The detailed methods and analyses were described in Liu et al. [99]. Differential metabolites were selected by considering both the fold change and the VIP (variable importance in projection) value of the OPLS-DA model. The screening criteria for significant differences were as follows:  $|\log_2(\text{fold change})| \geq 1$  and  $\text{VIP} \geq 1$ .

#### 4.19. Qualitative and quantitative analysis of metabolites

Qualitative and quantitative analyses of metabolites were conducted using the MRM mode of a QQQ mass spectrometer. The methods and analysis were described by Yang et al. [26].

Supplementary data to this article can be found online at <https://doi.org/10.1016/j.ijbiomac.2023.126762>.

#### CRediT authorship contribution statement

**Sufang Zhang:** Conceptualization, Methodology, Validation, Writing – original draft. **Bo Wang:** Data curation, Writing – review & editing. **Qian Li:** Investigation, Formal analysis. **Wenkai Hui:** Formal analysis. **Linjie Yang:** Methodology. **Zhihua Wang:** Data curation. **Wenjuan Zhang:** Validation. **Fengxia Yue:** Conceptualization. **Nian Liu:** Data curation. **Huiling Li:** Formal analysis. **Fachuang Lu:** Data curation. **Kewei Zhang:** Methodology. **Qingyin Zeng:** Writing – review & editing. **Ai-Min Wu:** Methodology, Validation, Writing – review & editing.

#### Declaration of competing interest

The authors declare that they have no conflicts of interest associated with this work.

#### Data availability

All relevant data can be found within the article or the supporting information.

#### Acknowledgements

We thank Weihui Li and Xianhai Zhao from South China Agricultural University for excellent technical assistance and discussions. We also thank Tsuyoshi Nakagawa from Shimane University for supplying the PGWB101 vector. This work was supported by National Key Research and Development Program of China (2022YFD2200102), National Natural Science Foundation of China (Grant Nos. 31870653 and 31670670), Key Project of Guangzhou Science and Technology Plan (201904020014), Natural Science Foundation of Guangdong Province, China (2020A1515011009).

#### References

- [1] H.Y. Zhao, J.H. Wei, Y.R. Song, Advances in research on lignin biosynthesis and its genetic engineering, *Zhi Wu Sheng Li Yu Fen Zi Sheng Wu Xue Xue Bao, Chinese* 30 (2004) 361–370 (PMID: 15627683).
- [2] S. Wolf, K. Hématy, H. Höfte, Growth control and cell wall signaling in plants, *Annu. Rev. Plant Biol.* 63 (2012) 381–407, <https://doi.org/10.1146/annurev-arplant-042811-105449>.
- [3] M.D. Venturas, J.S. Sperry, U.G. Hacke, Plant xylem hydraulics: what we understand, current research, and future challenges, *J. Integr. Plant Biol.* 59 (2017) 356–389, <https://doi.org/10.1111/jipb.12534>.
- [4] H. Li, Y. Xue, J. Wu, H. Wu, G. Qin, C. Li, J. Ding, J. Liu, L. Gan, M. Long, Enzymatic hydrolysis of hemicelluloses from *Miscanthus* to monosaccharides or xylooligosaccharides by recombinant hemicellulases, *Industrial Crops & Products* 79 (2016) (2016) 170–179, <https://doi.org/10.1016/j.indcrop.2015.11.021>.
- [5] A. Ziebell, E. Gjersing, M. Hinchee, R. Katahira, R.W. Sykes, D.K. Johnson, M.F. Davis, Downregulation of p-coumaroyl quinate/shikimate 3'-hydroxylase (*c3'h*) or cinnamate 4-hydroxylase (*c4h*) in eucalyptus *urophylla* × *eucalyptus grandis* leads to increased extractability, *Bioenergy Res.* 9 (2016) 1–9, <https://doi.org/10.1007/s12155-016-9713-7>.
- [6] M. Xie, J. Zhang, T.J. Tschaplinski, G.A. Tuskan, J.G. Chen, W. Muchero, Regulation of lignin biosynthesis and its role in growth-defense tradeoffs, *Front. Plant Sci.* 9 (2018) 1427, <https://doi.org/10.3389/fpls.2018.01427>.
- [7] N. Abdulrazzak, B. Pollet, J. Ehling, K. Larsen, C. Asnaghi, S. Ronseau, C. Proux, M. Erhardt, V. Seltzer, J.P. Renou, P. Ullmann, M. Pauly, C. Lapierre, D. Werck-Reichhart, A coumaroyl-ester-3-hydroxylase insertion mutant reveals the existence of nonredundant meta-hydroxylation pathways and essential roles for phenolic precursors in cell expansion and plant growth, *Plant Physiol.* 140 (2006) 30–48, <https://doi.org/10.1104/pp.105.069690>.
- [8] J. Wei, Y. Wang, H. Wang, R. Li, N. Lin, R. Ma, L. Qu, Y. Song, Pulping performance of transgenic poplar with depressed Caffeoyl-CoA O-methyltransferase, *Chin. Sci. Bull.* 53 (2008) 3553–3558, <https://doi.org/10.1007/s11434-008-0477-0>.
- [9] A. Day, G. Neutelings, F. Nolin, S. Grec, A. Habrant, D. Crönier, B. Maher, C. Rolando, H. David, B. Chabbert, S. Hawkins, Caffeoyl coenzyme a O-methyltransferase down-regulation is associated with modifications in lignin and cell-wall architecture in flax secondary xylem, *Plant Physiol. Biochem.* 47 (2009) 9–19, <https://doi.org/10.1016/j.jplphys.2008.09.011>.
- [10] X.P. Peng, S.L. Sun, J.L. Wen, W.L. Yin, R.C. Sun, Structural characterization of lignins from hydroxycinnamoyl transferase (HCT) down-regulated transgenic poplars, *Fuel* 134 (2014) 485–492, <https://doi.org/10.1016/j.fuel.2014.05.069>.
- [11] W. Pang, N. Dudareva, J.A. Morgan, C. Chapple, Genetic manipulation of lignocellulosic biomass for bioenergy, *Curr. Opin. Chem. Biol.* 29 (2015) 32–39, <https://doi.org/10.1016/j.cbpa.2015.08.006>.
- [12] J.K. Weng, C. Chapple, The origin and evolution of lignin biosynthesis, *New Phytol.* 187 (2010) 273–285, <https://doi.org/10.1111/j.1469-8137.2010.03327.x>.
- [13] X. Xu, D. Zhang, J. Hu, X. Zhou, X. Ye, K.L. Reichel, N.R. Stewart, R.D. Syrenne, X. Yang, P. Gao, W. Shi, C. Doeppke, R.W. Sykes, J.N. Burris, J.J. Bozell, M. Z. Cheng, D.G. Hayes, N. Labbe, M. Davis, C.N.J. Stewart, J.S. Yuan, Comparative genome analysis of lignin biosynthesis gene families across the plant kingdom, *BMC Bioinformatics* 10, S3 (2009), <https://doi.org/10.1186/1471-2105-10-S11-S3>.
- [14] J. de Vries, S. de Vries, C.H. Slamovits, L.E. Rose, J.M. Archibald, How embryophytic is the biosynthesis of phenylpropanoids and their derivatives in streptophyte algae? *Plant Cell Physiol.* 58 (2017) 934–945, <https://doi.org/10.1093/pcp/pcx037>.
- [15] S. de Vries, J.M.R. Fürst-Jansen, I. Irisarri, A.A. Dhabalia, T. Ischebeck, K. Feussner, I.N. Abreu, M. Petersen, I. Feussner, J. de Vries, The evolution of the phenylpropanoid pathway entailed pronounced radiations and divergences of enzyme families, *Plant J.* 107 (2021) 975–1002, <https://doi.org/10.1111/tpj.15387>.
- [16] W. Boerjan, J. Ralph, M. Baucher, Lignin biosynthesis, *Annu. Rev. Plant Biol.* 54 (2003) 519–546, <https://doi.org/10.1146/annurev.arplant.54.031902.134938>.
- [17] B. Hamberger, S. Bak, Plant P450s as versatile drivers for evolution of species-specific chemical diversity, *Philos. Trans. R. Soc. B* 368 (2013) 20120426, <https://doi.org/10.1098/rstb.2012.0426>.
- [18] R. Vanholme, B. De Meester, J. Ralph, W. Boerjan, Lignin biosynthesis and its integration into metabolism, *Curr. Opin. Biotechnol.* 56 (2019) 230–239, <https://doi.org/10.1016/j.copbio.2019.02.018>.
- [19] Y. Li, K. Wei, Comparative functional genomics analysis of cytochrome P450 gene superfamily in wheat and maize, *BMC Plant Biol.* 20 (2020) 93, <https://doi.org/10.1186/s12870-020-2288-7>.
- [20] B. Hamberger, M. Ellis, M. Friedmann, C. de Azevedo Souza, B.J. Barbazuk, C. Douglas, Genome-wide analyses of phenylpropanoid-related genes in *Populus trichocarpa*, *Arabidopsis thaliana*, and *Oryza sativa*: the *Populus* lignin toolbox and conservation and diversification of angiosperm gene families, *Can. J. Bot.* 85 (2007) 1182–1201, <https://doi.org/10.1139/B07-098>.
- [21] R. Shi, Y.H. Sun, Q. Li, S. Heber, R. Sederoff, V.L. Chiang, Towards a systems approach for lignin biosynthesis in *Populus trichocarpa*: transcript abundance and specificity of the monolignol biosynthetic genes, plant cell, *Physiology* 51 (2010) 144–163, <https://doi.org/10.1093/pcp/pcp175>.
- [22] Q. Sun, M. Foston, X. Meng, D. Sawada, S.V. Pingali, H.M. O'Neill, H. Li, C. E. Wyman, P. Langan, A.J. Ragauskas, R. Kumar, Effect of lignin content on changes occurring in poplar cellulose ultrastructure during dilute acid pretreatment, *Biotechnol. Biofuels* 7 (2014) 150, <https://doi.org/10.1186/s13068-014-0150-6>.

- [23] M.J. Chen, X.Q. Zhang, A. Matharu, E. Melo, R.M. Li, C.F. Liu, Q.S. Shi, Monitoring the crystalline structure of sugar cane bagasse in aqueous ionic liquids, *ACS Sustain. Chem. Eng.* 5 (2017) 7278–7283, <https://doi.org/10.1021/ACSSUSCHEMENG.7B01526>.
- [24] Y. Zhu, J. Huang, K. Wang, B. Wang, S. Sun, X. Lin, L. Song, A. Wu, H. Li, Characterization of lignin structures in *Phyllostachys edulis* (Moso bamboo) at different ages, *Polymers (Basel)*. 12 (2020) 187, <https://doi.org/10.3390/polym12010187>.
- [25] B. Zheng, Y. Zhu, S. Zheng, Y. Mo, S. Sun, J. Ren, Y. Li, A. Wu, H. Li, Upgrade the torrefaction process of bamboo based on autohydrolysis pretreatment, *Ind. Crop. Prod.* 166 (2021), 113470, <https://doi.org/10.1016/j.indcrop.2021.113470>.
- [26] H. Yang, N. Yi, S. Zhao, Z. Xiang, M.F. Qaseem, B. Zheng, H. Li, J.X. Feng, A.M. Wu, Characterization of hemicellulose in cassava (*Manihot esculenta Crantz*) stem during xylogenesis, *Carbohydr. Polym.* 264 (2021), 118038, <https://doi.org/10.1016/j.carbpol.2021.118038>.
- [27] M.L. Campos, J.H. Kang, G.A. Howe, Jasmonate-triggered plant immunity, *J. Chem. Ecol.* 40 (2014) 657–675, <https://doi.org/10.1007/s10886-014-0468-3>.
- [28] J. Ruan, Y. Zhou, M. Zhou, J. Yan, M. Khurshid, W. Weng, J. Cheng, K. Zhang, Jasmonic acid signaling pathway in plants, *Int. J. Mol. Sci.* 20 (2019) 2479, <https://doi.org/10.3390/ijms20102479>.
- [29] J. Mao, X. Xiong, Y. Lu, Advances in the regulation of plant stress response by jasmonic acid, *Chinese Journal of Bioprocess Eng.* 19 (2021) 1672–3678.
- [30] P. Kenrick, C.H. Wellman, H. Schneider, G.D. Edgecombe, A timeline for terrestrialization: consequences for the carbon cycle in the Palaeozoic, *Philos. Trans. R. Soc. B Biol. Sci.* 367 (2012) 519–536, <https://doi.org/10.1098/rstb.2011.0271>.
- [31] H. Renault, D. Werck-Reichhart, J.K. Weng, Harnessing lignin evolution for biotechnological applications, *Curr. Opin. Biotechnol.* 56 (2019) 105–111, <https://doi.org/10.1016/j.cobio.2018.10.011>.
- [32] J.K. Weng, J.A. Banks, C. Chapple, Parallels in lignin biosynthesis: a study in *Selaginella moellendorffii* reveals convergence across 400 million years of evolution, *Commun. Integr. Biol.* 1 (2008) 20–22, <https://doi.org/10.4161/cib.1.1.6466>.
- [33] M. Proctor, The diversification of bryophytes and vascular plants in evolving terrestrial environments, in: D.T. Hanson, S.K. Rice (Eds.), *Photosynthesis in Bryophytes and Early Land Plants*, 2014, pp. 59–77. New York.
- [34] Q. Zhao, Lignification: flexibility, biosynthesis and regulation, *Trends Plant Sci.* 21 (2016) 713–721, <https://doi.org/10.1016/j.tplants.2016.04.006>.
- [35] R. Zhong, D. Cui, Z.H. Ye, Secondary cell wall biosynthesis, *New Phytol.* 221 (2019) 1703–1723, <https://doi.org/10.1111/nph.15537>.
- [36] J. Ralph, K. Lundquist, G. Brunow, F. Lu, H. Kim, P.F. Schatz, J.M. Marita, R. D. Hatfield, S.A. Ralph, J.H. Christensen, W. Boerjan, Lignins: natural polymers from oxidative coupling of 4-hydroxyphenylpropanoids, *Phytochem. Rev.* 3 (2004) 29–60, <https://doi.org/10.1023/B:PHYT.0000047809.65444.a4>.
- [37] G. Peter, D. Neale, Molecular basis for the evolution of xylem lignification, *Curr. Opin. Plant Biol.* 7 (2004) 737–742, <https://doi.org/10.1016/j.pbi.2004.09.002>.
- [38] G. Schoch, S. Goepfert, M. Morant, A. Hehn, D. Meyer, P. Ullmann, D. Werck-Reichhart, CYP98A3 from *Arabidopsis thaliana* is a 3'-hydroxylase of phenolic esters, a missing link in the phenylpropanoid pathway, *Journal of Biology Chemistry* 276 (2001) 36566–36574, <https://doi.org/10.1074/jbc.M104047200>.
- [39] J. Raes, A. Rohde, J.H. Christensen, Y. Van de Peer, W. Boerjan, Genome-wide characterization of the lignification toolbox in *Arabidopsis*, *Plant Physiol.* 133 (2003) 1051–1071, <https://doi.org/10.1104/pp.103.026484>.
- [40] T. Yao, K. Feng, M. Xie, J. Barros, T.J. Tschaplinski, G.A. Tuskan, W. Muchero, J.G. Chen, Phylogenetic occurrence of the phenylpropanoid pathway and lignin biosynthesis in plants, *Frontiers in Plant Science*. (2021), 704697, doi:<https://doi.org/10.3389/fpls.2021.704697>.
- [41] H. Renault, M. De Marothy, G. Jonasson, P. Lara, D.R. Nelson, I. Nilsson, F. Andre, G. von Heijne, D. Werck-Reichhart, Gene duplication leads to altered membrane topology of a cytochrome P450 enzyme in seed plants, *Mol. Biol. Evol.* 34 (2017) 2041–2056, <https://doi.org/10.1093/molbev/msx160>.
- [42] S.L. Voelker, B. Lachenbruch, F.C. Meinzer, M. Jourdes, C. Ki, A.M. Patten, L. B. Davin, N.G. Lewis, G.A. Tuskan, L. Gunter, S.R. Decker, M.J. Selig, R. Sykes, M. E. Himmel, P. Kitin, O. Shevchenko, S.H. Strauss, Antisense down-regulation of 4CL expression alters lignification, tree growth, and saccharification potential of field-grown poplar, *Plant Physiol.* 154 (2010) 874–886, <https://doi.org/10.1104/pp.110.159269>.
- [43] R. Van Acker, J.C. Leplé, D. Aerts, V. Storme, G. Goeminne, B. Ivens, F. Légée, C. Lapierre, K. Piens, M.C. Van Montagu, N. Santoro, C.E. Foster, J. Ralph, W. Soetaert, G. Pilate, W. Boerjan, Improved saccharification and ethanol yield from field-grown transgenic poplar deficient in cinnamoyl-CoA reductase, *Proc. Natl. Acad. Sci.* 111 (2014) 845–850, doi:<https://doi.org/10.1073/pnas.1321673111>.
- [44] A. Chanoca, L. de Vries, W. Boerjan, Lignin engineering in Forest trees, *Frontiers in Plant Science*. 10 (2019) 912, <https://doi.org/10.3389/fpls.2019.00912>.
- [45] B. De Meester, B. Madariaga Calderón, L. de Vries, J. Pollier, G. Goeminne, J. Van Doorsselaere, M. Chen, J. Ralph, R. Vanholme, W. Boerjan, Tailoring poplar lignin without yield penalty by combining a null and haploinsufficient CINNAMOYL-CoA REDUCTASE2 allele, *Nat. Commun.* 11 (2020) 5020, <https://doi.org/10.1038/s41467-020-18822-w>.
- [46] P.M. Triziozi, H.W. Schmidt, C. Dervinis, M. Kirst, D. Conde, Simple, efficient and open-source CRISPR/Cas9 strategy for multi-site genome editing in *Populus tremula × alba*, *Tree Physiol.* 11 (2021) 2216–2227, <https://doi.org/10.1093/treephys/trab066>.
- [47] W.C. Yeap, N. Che Mohd Khan, N. Jamalludin, M.R. Muad, D.R. Appleton, H. Kulaveeraingam, An efficient clustered regularly interspaced short palindromic repeat (CRISPR)/CRISPR-associated protein 9 mutagenesis system for oil palm (*Elaeis guineensis*), *Frontiers in Plant Science*. 12 (2021), <https://doi.org/10.3389/fpls.2021.773656>.
- [48] X. Zhou, T.B. Jacobs, L.J. Xue, S.A. Harding, C.J. Tsai, Exploiting SNPs for biallelic CRISPR mutations in the crossing woody perennial *Populus* reveals 4-coumarate:CoA ligase specificity and redundancy, *New Phytol.* 208 (2015) 298–301, <https://doi.org/10.1111/nph.13470>.
- [49] S. Zhang, S. Wu, C. Hu, Q. Yang, T. Dong, O. Sheng, G. Deng, W. He, T. Dou, C. Li, C. Sun, G. Yi, F. Bi, Increased mutation efficiency of CRISPR/Cas9 genome editing in banana by optimized construct, *PeerJ.* 10 (2022), e12664, <https://doi.org/10.7717/peerj.12664>.
- [50] C. LeBlanc, F. Zhang, J. Mendez, Y. Lozano, K. Chatpar, V.F. Irish, Y. Jacob, Increased efficiency of targeted mutagenesis by CRISPR/Cas9 in plants using heat stress, *Plant J.* 2 (2018) 377–386, <https://doi.org/10.1111/tpj.13782>.
- [51] C. Feng, H. Su, H. Bai, R. Wang, Y. Liu, X. Guo, C. Liu, J. Zhang, J. Yuan, J. A. Birchler, F. Han, High-efficiency genome editing using a dmcl promoter-controlled CRISPR/Cas9 system in maize, *Plant Biotechnol. J.* 11 (2018) 1848–1857, <https://doi.org/10.1111/pbi.12920>.
- [52] J. Ordon, M. Bressan, C. Kretschmer, L. Dall’Osto, S. Marillonnet, R. Bassi, J. Stuttmann, Optimized Cas9 expression systems for highly efficient *Arabidopsis* genome editing facilitate isolation of complex alleles in a single generation, *Funct. Integr. Genomics* 1 (2020) 151–162, <https://doi.org/10.1007/s10142-019-00665-4>.
- [53] D. Fan, T. Liu, C. Li, B. Jiao, S. Li, Y. Hou, K. Luo, Efficient CRISPR/Cas9-mediated targeted mutagenesis in *Populus* in the first generation, *Sci. Rep.* 5 (2015) 12217, <https://doi.org/10.1038/srep12217>.
- [54] J.I. Kim, P.N. Ciesielski, B.S. Donohoe, C. Chapple, X.X. Li, Chemically induced conditional rescue of the reduced epidermal fluorescence8 mutant of *Arabidopsis* reveals rapid restoration of growth and selective turnover of secondary metabolite pools, *Plant Physiol.* 164 (2014) 584–595, <https://doi.org/10.1104/pp.113.229393>.
- [55] N.D. Bonawitz, J.I. Kim, Y. Tobimatsu, P.N. Ciesielski, N.A. Anderson, E. Ximenes, J. Maeda, J. Ralph, B.S. Donohoe, M. Ladisch, C. Chapple, Disruption of mediator rescues the stunted growth of a lignin-deficient *Arabidopsis* mutant, *Nature*. 509 (2014) 376–380, <https://doi.org/10.1038/nature13084>.
- [56] Y. Takeda, Y. Tobimatsu, S.D. Karlen, T. Koshiba, S. Suzuki, M. Yamamura, S. Murakami, M. Mukai, T. Hattori, K. Osakabe, J. Ralph, M. Sakamoto, T. Umezawa, Downregulation of p-COUMAROYL ESTER 3-HYDROXYLASE in rice lead to altered cell wall structures and improves biomass saccharification, *Plant J.* 95 (2018), <https://doi.org/10.1111/tpj.13988>.
- [57] I. El Houari, C. Van Beirs, H.E. Arents, H. Han, A. Chanoca, D. Opdenacker, J. Pollier, V. Storme, W. Steenackers, M. Quareshy, R. Napier, T. Beeckman, J. Friml, B. De Rybel, W. Boerjan, B. Vanholme, Seedling developmental defects upon blocking CINNAMATE-4-HYDROXYLASE are caused by perturbations in auxin transport, *New Phytol.* 230 (2021) 2275–2291, <https://doi.org/10.1111/nph.17349>.
- [58] H.D. Coleman, J.Y. Park, R. Nair, C. Chapple, S.D. Mansfield, RNAi-mediated suppression of p-coumaroyl-CoA 3'-hydroxylase in hybrid poplar impacts lignin deposition and soluble secondary metabolism, *the Proc. Natl. Acad. Sci.* 105 (2008) 4501–4506, <https://doi.org/10.1073/pnas.0706537105>.
- [59] X.P. Peng, J. Bian, S.Q. Yao, C.Y. Ma, J.L. Wen, Effects of P-Coumarate 3-hydroxylase downregulation on the compositional and structural characteristics of lignin and hemicelluloses in poplar wood (*Populus alba* x *Populus glandulosa*), *Front. Bioeng. Biotechnol.* 9 (2021), 790539, <https://doi.org/10.3389/fbioe.2021.790539>.
- [60] T. Hamann, M. Bennett, J. Mansfield, C. Somerville, Identification of cell-wall stress as a hexose-dependent osmosensitive regulator of plant responses, *Plant J.* 57 (2009) 1015–1026, <https://doi.org/10.1111/j.1365-313X.2008.03744.x>.
- [61] J.B. Fisher, G. Goldstein, T.J. Jones, S. Cordell, Wood vessel diameter is related to elevation and genotype in the Hawaiian tree *Metrosideros polymorpha* (Myrtaceae), *Am. J. Bot.* 94 (2007) 709–715.
- [62] J. Pittermann, The evolution of water transport in plants: an integrated approach, *Geobiology*. 8 (2010) 112–139, <https://doi.org/10.1111/j.1472-4669.2010.00232.x>.
- [63] H. Zhang, H. Liu, D.M. Niedzwiedzki, M. Prado, J. Jiang, M.L. Gross, R. E. Blankenship, Molecular mechanism of photoactivation and structural location of the cyanobacterial orange carotenoid protein, *Biochemistry*. 53 (2014) 13–19, <https://doi.org/10.1021/bi401539w>.
- [64] G.D. Farquhar, T.D. Sharkey, Stomatal conductance and photosynthesis, *Plant Physiol.* 33 (1982) 317–345, <https://doi.org/10.1146/annurev.pp.33.060182.001533>.
- [65] K. Maxwell, G.N. Johnson, Chlorophyll fluorescence-a practical guide, *J. Exp. Bot.* 51 (2000) 659–668, <https://doi.org/10.1093/jxb/51.345.659>.
- [66] W. Tezara, D. Martínez, E. Rengifo, A. Herrera, Photosynthetic responses of the tropical spiny shrub *Lycium nodosum* (Solanaceae) to drought, soil salinity and saline spray, *Annals of Botany Company Journals*. 92 (2003) 757–765, <https://doi.org/10.1093/aob/mcg199>.
- [67] M.D. Flowers, E.L. Fiscus, K.O. Burkey, F.L. Booker, J.J.B. Dubois, Photosynthesis, chlorophyll fluorescence, and yield of snap bean (*Phaseolus vulgaris* L.) genotypes differing in sensitivity to ozone, *Environmental & Experimental Botany*. 61 (2007) 190–198, <https://doi.org/10.1016/j.envexpbot.2007.05.009>.
- [68] L.Z. Mao, H.F. Lu, Q. Wang, M.M. Cai, Comparative photosynthesis characteristics of *Calycanthus chinensis* and *Chimonanthus praecox*, *Photosynthetica*. 45 (2007) 601–605, <https://doi.org/10.1007/s11099-007-0103-4>.
- [69] J. Xia, Y. Lang, Q. Zhao, P. Liu, L. Su, Photosynthetic characteristics of *Tamarix chinensis* under different groundwater depths in freshwater habitats, *Sci. Total Environ.* 761 (2021), 143221, <https://doi.org/10.1016/j.scitotenv.2020.143221>.

- [70] L. Lu, Y. Zhang, L. Li, N. Yi, Y. Liu, M.F. Qaseem, H. Li, A.M. Wu, Physiological and transcriptomic responses to nitrogen deficiency in *Neolamarckia cadamba*, Frontiers in Plant Science. 12 (2021), 747121, <https://doi.org/10.3389/fpls.2021.747121>.
- [71] X. Ma, L. Song, W. Yu, Y. Hu, Y. Liu, J. Wu, Y. Ying, Growth, physiological, and biochemical responses of *Camptotheca acuminata* seedlings to different light environments, Frontiers in Plant Science. 6 (2015) 321, <https://doi.org/10.3389/fpls.2015.00321>.
- [72] M. Zhang, L. Duan, X. Tian, Z. He, J. Li, B. Wang, Z. Li, Uniconazole-induced tolerance of soybean to water deficit stress in relation to changes in photosynthesis, hormones and antioxidant system, J. Plant Physiol. 164 (2007) 709–717, <https://doi.org/10.1016/j.jplph.2006.04.008>.
- [73] L. Zou, C. Pan, M.X. Wang, L. Cui, B.Y. Han, Progress on the mechanism of hormones regulating plant flower formation, Hereditas. 42 (2020) 739–751, <https://doi.org/10.16288/j.yczz.20-014>.
- [74] P.J. Davies, The plant hormones: Their nature, occurrence, and functions, in: P. J. Davies (Ed.), Plant Hormones, Springer, Dordrecht, 2010, pp. 1–15, [https://doi.org/10.1007/978-1-4020-2686-7\\_1](https://doi.org/10.1007/978-1-4020-2686-7_1).
- [75] T. Berleth, E. Scarpella, P. Prusinkiewicz, Towards the systems biology of auxin-transport-mediated patterning, Trends Plant Sci. 12 (2007) 151–159, <https://doi.org/10.1016/j.tplants.2007.03.005>.
- [76] D.C. Dinesh, L.I.A.C. Villalobos, S. Abel, Structural biology of nuclear auxin action, Trends Plant Sci. 21 (2016) 302–316, <https://doi.org/10.1016/j.tplants.2015.10.019>.
- [77] A.W. Woodward, B. Bartel, Auxin: regulation, action, and interaction, Ann. Bot. 95 (2005) (2005) 707–735, <https://doi.org/10.1093/aob/mci083>.
- [78] G. Hagen, Auxin signal transduction, Essays Biochem. 58 (2015) 1–12, <https://doi.org/10.1042/bse0580001>.
- [79] F. Ju, S. Liu, S. Zhang, H. Ma, J. Chen, C. Ge, Q. Shen, X. Zhang, X. Zhao, Y. Zhang, C. Pang, Transcriptome analysis and identification of genes associated with fruiting branch internode elongation in upland cotton, BMC Plant Biol. 19 (2019) 415, <https://doi.org/10.1186/s12870-019-2011-8>.
- [80] C. Fragnière, M. Serrano, E. Abou-Mansour, J.P. Métraux, F. L'Haridon, Salicylic acid and its location in response to biotic and abiotic stress, FEBS Lett. 585 (2011) (2011) 1847–1852, <https://doi.org/10.1016/j.febslet.2011.04.039>.
- [81] M. Rivas-San Vicente, J. Plasencia, Salicylic acid beyond defence: its role in plant growth and development, J. Exp. Bot. 62 (2011) 3321–3338, <https://doi.org/10.1093/jxb/err031>.
- [82] J. Lee, J. Nam, H.C. Park, G. Na, K. Miura, J.B. Jin, C.Y. Yoo, D. Baek, D.H. Kim, J. C. Jeong, D. Kim, S.Y. Lee, D.E. Salt, T. Mengiste, Q. Gong, S. Ma, H.J. Bohnert, S. S. Kwak, R.A. Bressan, P.M. Hasegawa, D.J. Yun, Salicylic acid-mediated innate immunity in *Arabidopsis* is regulated by SIZ1 SUMO E3 ligase, Plant J. 49 (2007) 79–90, <https://doi.org/10.1111/j.1365-313X.2006.02947.x>.
- [83] L. Gallego-Giraldo, L. Escamilla-Trevino, L.A. Jackson, R.A. Dixon, Salicylic acid mediates the reduced growth of lignin down-regulated plants, the, Proc. Natl. Acad. Sci. 108 (2011) 20814–20819, <https://doi.org/10.1073/pnas.1117873108>.
- [84] I. El Houari, W. Boerjan, B. Vanholme, Behind the scenes: the impact of bioactive phenylpropanoids on the growth phenotypes of *Arabidopsis* lignin mutants, Frontiers in Plant Science. 12 (2021), 734070, <https://doi.org/10.3389/fpls.2021.734070>.
- [85] S. Besseau, L. Hoffmann, P. Geoffroy, C. Lapierre, B. Pollet, M.M. Legrand, Flavonoid accumulation in *Arabidopsis* repressed in lignin synthesis affects auxin transport and plant growth, Plant Cell 19 (2007) 148–162, <https://doi.org/10.1105/tpc.106.044495>.
- [86] A. Fini, C. Brunetti, F.M. Di, F. Ferrini, M. Tattini, Stress-induced flavonoid biosynthesis and the antioxidant machinery of plants, Plant Signal. Behav. 6 (2011) 709–711, <https://doi.org/10.4161/psb.6.5.15069>.
- [87] D.E. Brown, A.M. Rashotte, A.S. Murphy, J. Normanly, B.W. Tague, W.A. Peer, L. Taiz, G.K. Muday, Flavonoids act as negative regulators of auxin transport in vivo in *arabidopsis*, Plant Physiol. 126 (2001) 524–535, <https://doi.org/10.1104/pp.126.2.524>.
- [88] C.S. Buer, F. Kordbacheh, T.T. Truong, C.H. Hocart, M.A. Djordjevic, Alteration of flavonoid accumulation patterns in transparent testa mutants disturbs auxin transport, gravity responses, and imparts long-term effects on root and shoot architecture, Planta. 238 (2013) 171–189, <https://doi.org/10.1007/s00425-013-1883-3>.
- [89] L. Wang, W. Lu, L. Ran, L. Dou, S. Yao, J. Hu, D. Fan, C. Li, K. Luo, R2R3-MYB transcription factor MYB6 promotes anthocyanin and proanthocyanidin biosynthesis but inhibits secondary cell wall formation in *Populus tomentosa*, Plant J. 99 (2019) 733–751, <https://doi.org/10.1111/tpj.14364>.
- [90] K.J. Livak, T.D. Schmittgen, Analysis of relative gene expression data using real-time quantitative PCR and the  $2^{-\Delta\Delta CT}$  method, Methods. 25 (2001) 402–408, <https://doi.org/10.1006/meth.2001.1262>.
- [91] X. Ma, Y.G. Liu, CRISPR/Cas9-based multiplex genome editing in monocot and dicot plants, Curr. Protoc. Mol. Biol. 115 (2016), <https://doi.org/10.1002/cpmb.10>, 31.6.1-31.6.21.
- [92] T. Nakagawa, T. Kurose, T. Hino, K. Tanaka, M. Kawamukai, Y. Niwa, K. Toyooka, K. Matsuo, T. Jinbo, T. Kimura, Development of series of gateway binary vectors, pGWBs, for realizing efficient construction of fusion genes for plant transformation, J. Biosci. Bioeng. 104 (2007) 34–41, <https://doi.org/10.1263/jbb.104.34>.
- [93] S. Li, Y.J. Lin, P. Wang, B. Zhang, M. Li, S. Chen, R. Shi, S. Tunlaya-Anukit, X. Liu, Z. Wang, X. Dai, J. Yu, C. Zhou, B. Liu, J.P. Wang, V.L. Chiang, W. Li, The AREB1 transcription factor influences histone acetylation to regulate drought responses and tolerance in *Populus trichocarpa*, Plant Cell 31 (2019) 663–686, <https://doi.org/10.1105/tpc.18.00437>.
- [94] S. Timm, M. Mielewczik, A. Florian, S. Frankenbach, A. Dreissen, N. Hocken, A. R. Fernie, A. Walter, H. Bauwe, High-to-low CO<sub>2</sub> acclimation reveals plasticity of the photorespiratory pathway and indicates regulatory links to cellular metabolism of *Arabidopsis*, PLoS One 7 (2012), e42809, <https://doi.org/10.1371/journal.pone.0042809>.
- [95] B. Dai, C. Chen, Y. Liu, L. Liu, M.F. Qaseem, J. Wang, H. Li, A.M. Wu, Physiological, biochemical, and transcriptomic responses of *neolamarckia cadamba* to aluminum stress, Int. J. Mol. Sci. 21 (2020) 9624, <https://doi.org/10.3390/ijms21249624>.
- [96] A. Sluiter, B. Hames, R. Ruiz, C. Scarlata, J. Sluiter, D. Templeton, D. Crocker, Determination of structural carbohydrates and lignin in biomass, Laboratory Analytical Procedure. 1617 (2008) 1–16, in: [http://www.nrel.gov/biomass/analytical\\_procedures.html](http://www.nrel.gov/biomass/analytical_procedures.html).
- [97] J.B. He, X.H. Zhao, P.Z. Du, W. Zeng, C.T. Beahan, Y.Q. Wang, H.L. Li, A. Bacic, A. M. Wu, KNAT7 positively regulates xylan biosynthesis by directly activating IRX9 expression in *Arabidopsis*, J. Integr. Plant Biol. 60 (2018) 514–528, <https://doi.org/10.1111/jipb.12638>.
- [98] A. Rigal, S.M. Doyle, S. Robert, Live cell imaging of FM4-64, a tool for tracing the endocytic pathways in *Arabidopsis* root cells, Methods Mol. Biol. 1242 (2015) 93–103, [https://doi.org/10.1007/978-1-4939-1902-4\\_9](https://doi.org/10.1007/978-1-4939-1902-4_9).
- [99] M. Liu, Q. Du, P. Liu, J. Q., H. Du, L. Wang, Characterization of new mutant *Eucommia ulmoides* constituents in the discoloration during growing, Wood Research. 65 (2020) 415–422, <https://doi.org/10.37763/wr.1336-4561/65.3.415422>.